Synaptic inputs to physiologically defined turtle retinal ganglion cells

JAY F. MULLER,[1] JOSEF AMMERMÜLLER,[2] RICHARD A. NORMANN[3,1] AND HELGA KOLB[1]
[1]Department of Physiology, University of Utah School of Medicine, Salt Lake City
[2]Department of Neurobiology, University of Oldenburg, Oldenburg, Germany
[3]Department of Bioengineering, University of Utah, Salt Lake City

Abstract

Two physiologically distinct, HRP-marked turtle retinal ganglion cells were examined for their morphology, GABAergic, glycinergic, and bipolar cell synaptic inputs, using electron-microscopic autoradiography and postembedding immunocytochemistry. One cell was a *color-opponent, transient ON/OFF* ganglion cell. Its center response to *red* was a sustained hyperpolarization, and its center response to *green* was a depolarization with increased spiking at onset. The HRP-injected cell most resembled G6, from previous Golgi-impregnation studies (Kolb, 1982; Kolb et al., 1988). It was a narrow-field bistratified cell, whose two broad dendritic strata peaked at approximately levels L20-25 (sublamina *a*) and L60 (sublamina *b*) of the inner plexiform layer. Bipolar cell synapses onto G6 were found evenly distributed between its distal and proximal dendritic strata, spanning L20-75. These inputs probably originated from several different bipolar cells, reflecting the complexity of the center response. GABAergic inputs were found onto both the distal and proximal strata, from near L20-L85. Only a few glycinergic inputs, confined to dendrites at L50-70, were observed.

A second ganglion cell type that we physiologically characterized and HRP-injected had *sustained ON-center, sustained OFF-surround* responses. Two examples were studied; both were bistratified in sublamina *b*, near L60-70 and L85-100, with branches up to near L40. They resembled G10, from previous Golgi-impregnation studies (Kolb, 1982; Kolb et al., 1988). One cell was partially reconstructed to look at the distributions of GABAergic and glycinergic amacrine cell, and bipolar cell inputs. Although synapses from bipolar cells were equally divided between the two major dendritic strata of G10, the inputs to the distal stratum were close to the soma, and the inputs to the more proximal stratum were on the peripheral dendrites. This arrangement may reflect input from two distinct types of ON-bipolar cell. GABAergic and glycinergic inputs to G10 costratified to both strata and to the distal branches; but where glycinergic inputs were found distributed throughout the arbor, GABAergic inputs appeared to be confined to peripheral dendrites. We hypothesize on the neural elements involved and the circuitry that may underlie the physiologically recorded receptive fields of these two very different ganglion cell types in the turtle retina.

Keywords: Neuronal circuitry, Intracellular recording, γ-aminobutyric acid (GABA), Glycine, Autoradiography, Immunocytochemistry

Introduction

A variety of ganglion cells have been described morphologically and physiologically in turtle retina. Recent anatomical studies, using Golgi impregnation in two related turtle species (Kolb, 1982; Kolb et al., 1988), have described over 20 different ganglion cell types, varying in somatic and dendritic morphology, dendritic branching patterns, expanse, and stratification in the inner plexiform layer (IPL). Electrophysiological recordings have found representatives of the general classes of ON-center, OFF-center, and ON/OFF ganglion cells (Lipetz & Hill, 1970;

Bowling, 1980; Jensen & DeVoe, 1983), as well as chromatically opponent, directionally selective, wavelength, orientation and movement sensitive, and temporally coded ganglion cells, favoring fast or slow movement (Lipetz & Hill, 1970; Bowling, 1980; Marchiafava & Wagner, 1981; Jensen & DeVoe, 1982, 1983; Marchiafava, 1983; Adolph, 1989; Granda & Fulbrook, 1989). However, little is known about the synaptic inputs to any of the morphologically or physiologically characterized cells in the turtle retina. In fact, we have a paucity of information on the underlying neural circuits that define physiological responses of ganglion cells in vertebrate retinas in general.

In the present paper, two clearly distinct physiological types of turtle retinal ganglion cell are studied by electron microscopy with cytochemical labeling for γ-aminobutyric acid (GABA) and glycine, to determine their underlying synaptology: one, a

sustained ON-center cell with a spatially opponent surround, and the other, a transient ON/OFF cell with a color-opponent center. We anticipated that differences in synaptic input might give us clues as to how receptive-field components such as ON and OFF transients, color opponency, and sustained center and opponent surround responses are generated at the ganglion cell level.

Materials and methods

Intracellular recording and HRP injection

Adult turtles (*Pseudemys scripta elegans*), 20–25 cm in length were anesthetized with ketamine (Vetalar, Aveco, Fort Dodge, IA), and prepared for physiological recording from an eyecup, using methods adapted from Ammermüller and Weiler (1988). For the preparations described herein, the anterior part of the eye was removed, but the eyecup was left in the pithed cranium so that the optic nerve remained intact. The orbits were filled with Vaseline or Gelfoam to stabilize the eyecup. After vitrectomy, the preparation was placed in the recording chamber, grounded, and superfused with oxygenated turtle Ringers solution: 110 mM NaCl, 2.6 mM KCl, 2 mM $MgCl_2$, 2 mM $CaCl_2$, 10 mM D-glucose, and 22 mM $NaHCO_3$. The pH of the solution was maintained at 7.4 by constant bubbling with 95% $O_2/5\%$ CO_2. Radially placed Kimwipe wedges helped maintain flow across the vitreal surface. After aligning and focusing a test spot, the eyecup was left to dark adapt for 15 min.

Intracellular recordings were done with glass microelectrodes filled with 4% horseradish peroxidase (HRP) in 0.05 M tris and 0.4 M KCl at pH 8.6, with resistances ranging from 600–1000 MΩ. Positive feedback pulses were used to facilitate cell impalement. HRP was injected with a train of 10–20 nA positive constant current pulses of 0.5-s duration. When the current decreased, however, sometimes 1- or 2-s pulses were used. Injections usually lasted 5–10 min. After each pulse and following the injection period, the amplifier was switched to voltage-recording mode to ascertain that we were in the original cell and that it was light responsive. Cells were stimulated with circular spots and annuli of different inner diameters (i.d.), centered around the microelectrode, and attenuated by neutral density filters. Red (694 nm), green (514 nm), and blue (450 nm) spots and annuli were produced with interference type band-pass filters. Intensity response series and receptive-field estimates were generally done with attenuated white spots and annuli. Approximate intensities at different attenuation levels are listed in the legend for Fig. 3. A slit projected at 2.4 nm x 0.2 mm and a grating of 3.1 cycles/mm, both at a velocity of 1.7 mm/s, were used to test for directional bias or selectivity. To facilitate locating the HRP-injected cells, we made a schematic map of the injection sites, using the visual streak and optic nerve head as landmarks.

Isolated retina: incubation in [³H]-neurotransmitters

Following the recording sessions, the preparations were left in the dark for 30 min, under superfusion, to allow time for the last HRP injections to transport to the peripheral dendrites, and to dark adapt the eye. The retinas were then isolated, delicately freeing as much pigment epithelium as possible; notches were made in the periphery for orientation landmarks. Isolated whole retinas were incubated for 15 min in 50-μl droplets of micromo-

lar concentrations of [³H]-glycine (S.A.: 10–40 Ci/mmole) obtained from ICN (Costa Mesa, CA), or [³H]-GABA (S.A.: 25–40 Ci/mmole) with 1 mM nipecotic acid added (Marc, 1989; Muller & Marc, 1990), in a moist, oxygenated environment. After a gentle 30-s saline rinse, the retinas were fixed in freshly prepared fixative: 1% paraformaldehyde, 2.5% glutaraldehyde, 0.012% calcium chloride, and 3% sucrose in 100 mM sodium cacodylate buffer, at pH 7.4, for 2 h. The retinas were then rinsed several times in 0.16 M sodium cacodylate and left overnight in 0.16 M sodium cacodylate with 5% sucrose.

As previously described in goldfish (Marc et al., 1978; Marc, 1986, 1989; Muller & Marc, 1990), and alluded to in turtle (Tachibana & Kaneko, 1984), the high density of GABA uptake sites in the outer plexiform layer (of retinas with GABAergic horizontal cells) and the proximal inner plexiform layers act as spatial buffers. When micromolar concentrations of [³H]-GABA are used, these border areas act as a sink, drastically reducing the ligand concentration available for uptake by terminals in the intervening layers. Under these conditions, only amacrine cells that project to the proximal IPL are well-labeled. When added to the incubation media, unlabeled GABA or nipecotic acid, a competitive inhibitor of GABA uptake with a similar Km (Michaelis–Menten constant), can reversibly occupy uptake sites, reducing label retention at the border areas, making it more available to the distal IPL. This allows all GABAergic amacrine cells to be labeled (Marc, 1989; Muller & Marc, 1990). A test series was done beforehand, incubating quartered retinas (Muller & Marc, 1990) to determine the best concentration of nipecotic acid to add to the micromolar concentrations of [³H]-GABA for good label distribution but adequate grain density (Marc, 1989). As with goldfish, 1 mM nipecotic acid was found to be an effective concentration for quarters of turtle retina (Fig. 1A). Therefore all [³H]-GABA uptake preparations described herein were incubated with 1 mM nipecotic acid added.

Histology: cell identification

After the overnight sucrose-buffer rinse, whole retinas were rinsed with buffer and developed for HRP with diaminobenzidine tetrachloride (DAB). Retinas were presoaked with filtered 0.1% DAB in 0.16 M sodium cacodylate for 45 min, with mild agitation. Hydrogen peroxide was then added, to a final concentration of 0.02–0.03%, for an additional 45 min. After several buffer rinses, retinas were spread on a slide and cleared briefly with buffered glycerol, and examined under a microscope to search for successfully HRP-labeled cells. Preliminary wholemount sketches were made of cells in areas that might be difficult to read after osmium postfixation. Retinas were rinsed thoroughly, at least five changes of buffer over an hour period, with agitation, to free the tissue of glycerol.

To maintain flatness during postfixation and dehydration, retinas were placed in a sandwich: two layers of Whatman #50 filter paper around the retina, secured between plastic coverslips, each with small holes punched near the center, bound with a small rubber band. The holes in the coverslips were essential to let osmium tetroxide penetrate the turtles' relatively thick central retinas, the site of most of the injected cells. All subsequent steps were done with mild agitation. Sandwiched retinas were placed in 1% osmium tetroxide in 0.16 M sodium cacodylate for 45 min, after which they were further incubated in buffered 1% osmium tetroxide with 1.5% potassium ferricyanide (Muller & Marc, 1990). After buffer rinses, dehydration

was begun with 15 min each in 50% and 70% ethanol. Then the sandwiched retinas were stained *en bloc* in filtered 2% uranyl acetate in 70% ethanol for 1 1/2 h. The dehydration was continued stepwise after two rinses in 70% ethanol. After 15 min in 100% ethanol, the coverslips were removed and the retina transferred to fresh 100% ethanol, further dehydrated and embedded in a soft Polybed 812 (Polysciences, Warrington, PA) mixture (Muller & Marc, 1984, 1990). Retinas were placed on a slide between plastic coverslips, weighted, and polymerized. Where possible, HRP-labeled cells were drawn in wholemount with camera lucida, with a Zeiss 40× oil immersion lens. Regions containing labeled cells were then excised from the wholemount, remounted, and cut in serial 40-μm vertical sections, with an AO 812 rotary microtome. Cells were then reconstructed with camera lucida from the 40-μm sections, using a Zeiss 100× objective, and regions were chosen for remounting for future ultrastructural and cytochemical analysis. Ganglion cells were named based on previous Golgi-impregnation studies (Kolb, 1982; Kolb et al., 1988).

Autoradiography

Retinal regions near labeled cells were tested for [³H]-neurotransmitter uptake efficacy using light-microscopic autoradiography (LMARG) of 1-μm semithin sections, as previously described (Marc et al., 1978; Muller & Marc, 1990). To accentuate IPL strata, exposure times for LMARG were from 10 days to 4 weeks (Fig. 1); when colabeled with immunocytochemistry (Fig. 2), the intervals were 3–7 days. Once the approximate exposure times for electron microscopy were decided for each preparation, serial or near-serial sections were cut, with a glass or diamond knife on a Sorvall MT2B ultramicrotome. Silver-gold thin sections were collected on slot grids with support films of either 0.6% parlodion in n-pentyl acetate or 0.6–0.7% formvar in chloroform. For electron-microscopic (EM) autoradiography, sections were then stained with uranyl acetate and Luft's lead citrate and given a moderately heavy carbon coat. Grids were then individually coated with L4 emulsion (Polysciences) using wire loops, mounted on slides, and exposed in the dark at 4°C for 5–14 weeks, depending on the preparation, and developed with phenidon (Bouteille, 1976; Marc et al., 1978; Muller & Marc, 1990).

Immunocytochemistry

Postembedding immunocytochemistry was performed at the light- and electron-microscopic levels, using antisera prepared against GABA and glycine, as glutaraldehyde modified, bovine serum Albumin conjugates (Pourcho & Owczarzak, 1989). Antibodies were generously supplied by Dr. Pourcho or purchased from Incstar Corporation (Stillwater, MN). Methods used for both light- and electron-microscopic immunostaining were generally adapted from Pourcho and Owczarzak (1989). However, except for those preparations represented by Figs. 1B, 1E, and 1F, all retinas were fixed as described above, in the "Isolated retina" section. Primary antibody dilutions for light microscopy were 1:1000 for anti-GABA and 1:500 for anti-glycine, when using a fixative containing 4% paraformaldehyde and 0.5% glutaraldehyde. Dilutions of 1:500 for anti-GABA and 1:100 for anti-glycine worked better, when using our standard fixative, for both light-microscopic and electron-microscopic preparations.

To test for correspondence between autoradiographic and immunocytochemical markers for GABAergic and glycinergic neurons, and separability of GABAergic and glycinergic label, we combined the techniques in a light-microscopic double label. Immunostaining was followed by emulsion coating and exposure for autoradiography (Fig. 2). To estimate label specificity at the ultrastructural level, the inner nuclear layer was surveyed (Muller & Marc, 1990). Adapting previously established statistical criteria for ultrastructural grain localization (Kelly & Weitsch–Dick, 1978), we used a criterion grain density ratio of 5:1, with a threshold of 4 grains per 1 μm² labeled terminal. Similar to previous preparations, in goldfish retina (Muller & Marc, 1990), the estimated signal-to-noise ratios for [³H]-glycine and [³H]-GABA plus 1 mM nipecotic acid label for EM autoradiography were approximately 30:1 and 20:1, respectively. For postembedding immunocytochemistry and localization of immuno-gold, the estimated signal-to-noise ratios for most preparations were from 5:1–9:1; those that did not meet the 5:1 criterion were eliminated from analysis. When seeking GABAergic or glycinergic inputs onto HRP-labeled ganglion cell profiles, using autoradiographic or immunocytochemical markers as the second label, serial section analysis was critical. All double-labeled synapses counted herein were followed serially, most for three or more sections, to ascertain both labels and synaptic contact.

The two systems used in this report for describing where dendrites stratify in the IPL are the well-known sublamina *a/b* model, delineating OFF-center and ON-center pathway components (Famiglietti et al., 1977; Nelson et al., 1978), and the percent level in the IPL, with L0 and L100 as the amacrine cell layer and ganglion cell layer borders, respectively (Marchiafava & Weiler, 1980; Weiler, 1981; Eldred & Karten, 1983; Marc, 1986; Hurd & Eldred, 1989). The basis for establishing the sublamina *a/b* border in vertebrate retinas has been where dye-injected ON- and OFF-center ganglion cells and bipolar cells stratify (Famiglietti et al., 1977; Nelson et al., 1978; Hare et al., 1986). In turtle we have too few dye-injected ganglion cells to establish a border; however, Weiler (1981), based on physiologically recorded and procion yellow-injected bipolar cells, found ON-bipolar cells terminated between L40 and L100 and OFF-bipolar cells had their distal-most axon terminals between L0 and L50. Two of Weiler's reconstructed bipolar cells correlated to Kolb's B4 and B6 (Kolb, 1982; Kolb et al., 1986). Using B4 and B6 as exemplars for OFF- and ON-bipolar cells, respectively, the sublamina *a/b* border appears to be near L40. Occasional references are made herein to IPL strata: S1-5, to correlate our data to previous work (Kolb, 1982; Kolb et al., 1988). Kolb (1982) divided the turtle IPL into five equal subdivisions, so, for example, L40 is equivalent to the S2/3 border.

Results

Light-microscopic autoradiography and immunocytochemistry

Since both electron-microscopic autoradiography and immunocytochemistry, for both GABA and glycine, are used in this study to look at IPL synaptology, correspondence between the techniques and distinction between markers are important issues. Figures 1 and 2 are light microscopic examples of these preparations, meant to give a broad view of the markers' labeling patterns. As shown in Figs. 1A–F, there is good agreement between techniques, when labeling for a given neurotransmitter.
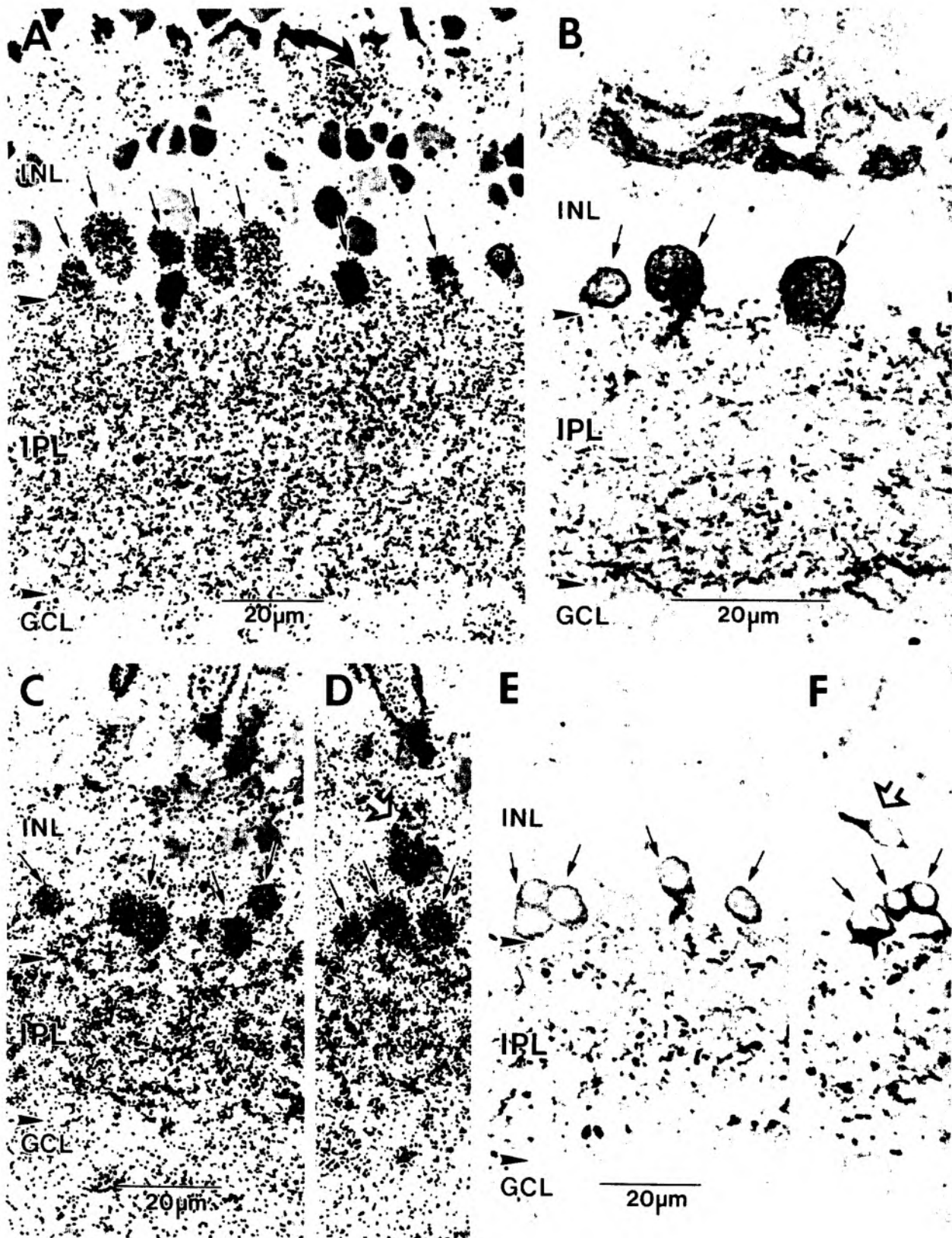
Fig. 1. GABAergic and glycinergic labels: light-microscopic autoradiography and immunocytochemistry. A: [^{3}H]-GABA uptake, light-microscopic autoradiography. Small arrows indicate GABA-labeled amacrine cells. Unlabeled small, pyriform amacrine cells (possibly glycinergic) marked with asterisks. GABA-labeled horizontal cell body indicated by curved, black arrow. Arrowheads frame the inner plexiform layer (IPL), at the ganglion cell layer (GCL) and amacrine cell layer (ACL) borders. B: GABA-immunoreactive amacrine cells (small arrows) and horizontal cell axon terminals (curved white arrow). C,D: [^{3}H]-glycine uptake, light-microscopic autoradiography. Glycine-labeled amacrine cells (small arrows) and unlabeled amacrine cells (asterisks) are indicated. A glycine-accumulating bipolar cell (open arrow) is shown in D. E,F: Glycine-immunoreactive amacrine cells (small arrows) and a glycine-immunoreactive bipolar cell (open arrow) in F. Note, the thickness of the IPL varies with eccentricity.

412
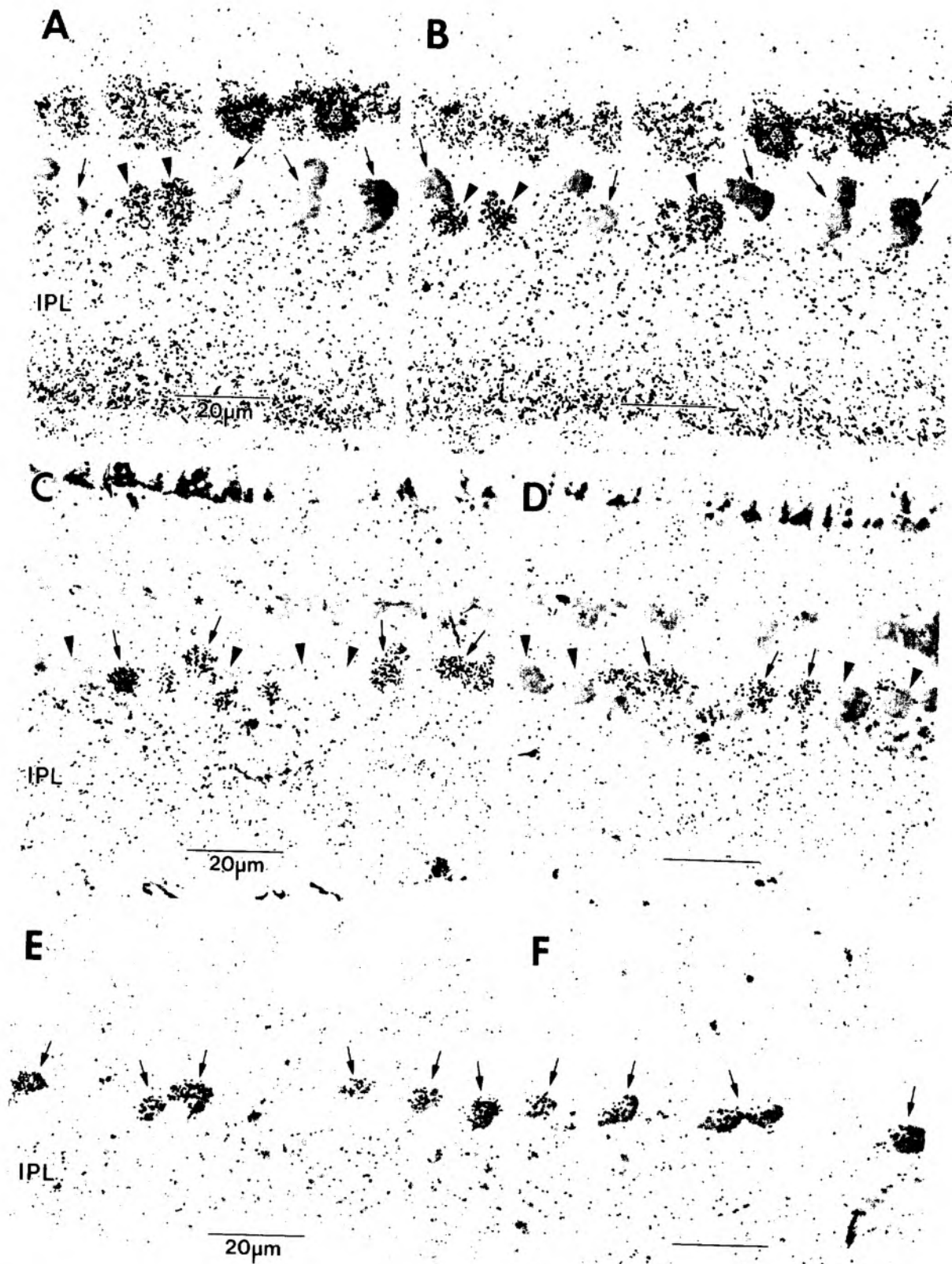
Fig. 2. Light-microscopic double label. In A–F, small arrows indicate glycine-labeled amacrine cells, arrowheads indicate GABA-labeled amacrine cells, and asterisks mark GABA-labeled horizontal cells. Horizontal cells, although not discussed further in this report, are used here as a GABAergic label standard. A,B: Serial light micrographs of glycine immunoreactivity with [^{3}H]-GABA uptake and autoradiography. Several amacrine cells are well-marked for GABA (arrowheads); glycine-immunoreactive amacrine cells (small arrows) are virtually free of silver grains. C,D: Light micrographs of GABA immunoreactivity with [^{3}H]-glycine uptake and autoradiography. GABA-labeled amacrine cells and horizontal cells show no evidence of glycine uptake. A separate population of amacrine cells are labeled with silver grains for [^{3}H]-glycine uptake. E,F: Colocalization of glycine immunoreactivity and [^{3}H]-glycine uptake. Silver grains are concentrated on immunoreactive neurons. No other cell bodies show grain localization.

413

Figures 1A and 1B compare [³H]-GABA uptake and autoradiography with GABA immunoreactivity. Similarly, autoradiographic localization of [³H]-glycine uptake (Figs. 1C and 1D) is compared with glycine immunoreactivity (Figs. 1E and 1F). Both GABA and glycine label a diversity of amacrine cells in the two proximal tiers of the inner nuclear layer (arrows). In general, GABA labels more large cells in the first tier and glycine more small cells in the second tier. GABA labels a population of horizontal cells (H1) and their axon terminals (Figs. 1A and 1B, black and white curved arrows, respectively). Glycine does not label horizontal cells, but a number of bipolar cells show evidence of glycine uptake and glycine immunoreactivity (Figs. 1D, and 1F, open arrows). Similar findings have been described previously in turtle (Eldred & Cheung, 1989; Hurd & Eldred, 1989), as well as reported in other species (Marc et al., 1978; Marc, 1985, 1986, 1989; Marc & Liu, 1985; Yazulla, 1986; Pourcho & Goebel, 1987; Hendrickson et al., 1988; Yazulla & Studholme, 1990). Also common to other vertebrates, GABAergic and glycinergic strata overlap, spanning most of the IPL (Marc & Lam, 1981; Kleinschmidt & Yazulla, 1984; Marc, 1985; Marc & Liu, 1985; Marc, 1986; Mariani & Caserta, 1986; Mosinger et al., 1986; Pourcho & Goebel, 1987; Hendrickson et al., 1988; Muller & Marc, 1990). Sections of moderately labeled immunocytochemical preparations were chosen, so that the dominant strata could better be compared to autoradiographic uptake patterns.

Some retinas, however, had regional variations with respect to how well the distal strata were labeled. Figure 1A is representative of preparations where quartered retinas were incubated in [³H]-GABA and nipecotic acid, while Fig. 2A is a sample from incubated whole retinas. The main advantage of incubating retinal portions over whole retinas may be more uniform access to factors in the incubation media. Retinal folding and vitreal pooling, in whole retinas, may impede diffusion and reduce access to moist oxygen flow, particularly at the vitreal surface. These additional barriers might reduce the concentration or transport efficiency of available [³H]-GABA at the retina's proximal border, thereby compromising label redistribution by nipecotic acid, so that some GABAergic amacrine cells label less intensely (see Methods).

Double label

To demonstrate the general non-colocalization of GABAergic and glycinergic markers in turtle, GABAergic uptake was combined with glycinergic immunoreactivity and glycinergic uptake was combined with GABAergic immunoreactivity (Fig. 2). In the first case (Figs. 2A and 2B), glycine-immunoreactive (arrows) and [³H]-GABA accumulating amacrine cells (arrowheads) are easily distinguishable, as are non-glycine-immunoreactive, [³H]-GABA accumulating horizontal cells (asterisks). In Figs. 2C and 2D, it is apparent that GABA-immunoreactive amacrine cells (arrowheads) and horizontal cells (asterisks) are virtually free of silver grains, whereas distinct populations of amacrine cells show clear autoradiographic evidence of glycine uptake (arrows).

The results presented in Figs. 2A and 2B differ somewhat from the preparation shown in Fig. 1A, in that the distal IPL strata for GABA labeled less densely, in this region of the retina. This means that GABA-accumulating amacrine cells arborizing in sublamina *a* would appear more lightly labeled. Even so, the two preparations presented in Figs. 2A–2D, taken

together, show virtually no overlap between GABAergic and glycinergic systems. Apparently, the sum of these two systems makes up the majority of amacrine cells. It is also clear that the correspondence between autoradiography and immunocytochemistry was excellent, as exemplified by colocalization of glycinergic markers (Figs. 2E and 2F).

Color-coded ON/OFF ganglion cell (G6)

Physiological recording

Initial stimulation with dim white 0.5-s flashes revealed an ON/OFF ganglion cell, with single or short bursts of spikes at onset and offset, and little spontaneous activity. A series of white spots of increasing diameter and two annuli of different inner diameters were used as stimuli to estimate the receptive-field's diameter and test for spatial opponency. A 210-μm-diam spot (spot 1, see Fig. 3B) elicited a clear ON/OFF response. With progressively larger spots there was increasing hyperpolarization and decreased spike amplitude. The annulus of 0.92 mm i.d. (annulus 12) elicited a sustained hyperpolarization (Fig. 3B). Apparently, this ON/OFF ganglion cell has a receptive-field center not much larger than 200 μm (and perhaps smaller), i.e. roughly the size of its compact dendritic arbor; and it has a spatially opponent surround.

We tested for color coding with red (694 nm), green (514 nm), and blue (450 nm) spots at different intensities (see Fig. 3B). Results with 210-μm spot (spot 1) stimuli are presented, as they gave the clearest responses, with the highest amplitude spikes. The responses to red and green flashes were quite distinct. The ganglion cell's response to red-light onset was clearly a sustained hyperpolarization, whereas the response to green-spot onset was a transient depolarization with a sustained depolarizing component which was most evident at a lower intensity (−2.5 N.D. attenuation). This intensity was below the apparent spike threshold, as the transient component was not visible (see Fig. 3B). The transient depolarization elicited by green at −1.5 N.D. attenuation was accompanied by a discernable increase in spike number. The differences between the responses to red and green onset can be most clearly seen at −1.5 N.D. and −0.5 N.D. attenuation (see Fig. 3B). At offset, both red and green appeared to elicit or contribute to a transient depolarization or spike (Fig. 3B: red, N.D. −2.5, −1.5; green, N.D. −1.5, −0.5). At higher intensities (−0.5 N.D.), it appears that red-induced hyperpolarization was sustained enough to suppress the OFF depolarization. Green, equally attenuated (−0.5 N.D.), elicited a response more like that of white light, with a more hyperpolarized sustained component, probably because it surpassed the threshold for activating the red-signal pathways (Fig. 3B). The response to blue, with −0.5 N.D. attenuation, was clearly ON/OFF, and appeared qualitatively similar to the responses to green. The results of our color annulus series were equivocal, as the light response began to deteriorate when these measurements were made. Therefore, the only clear information we have about the surround is its sustained hyperpolarization to white annuli and large white spots, i.e. spatial opponency (Fig. 3B, spot series).

Morphology: cell identification

The above-described HRP-filled ganglion cell was located in a retinal area that was too optically dense for a detailed drawing in wholemount. Therefore, the cell was reconstructed with camera lucida, from a series of five vertical 40-μm sections.

G6

A

B
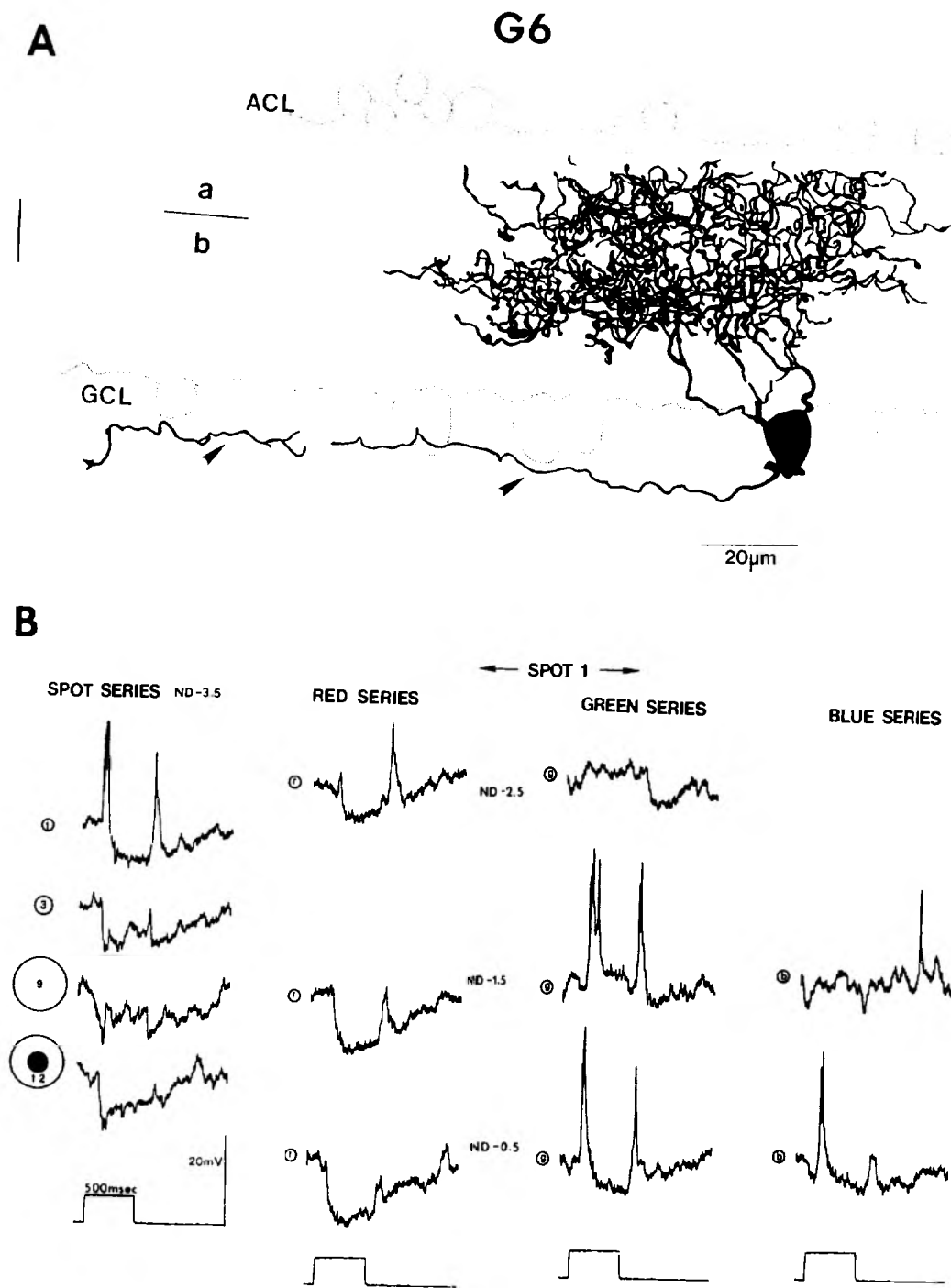
Fig. 3. Color-opponent, transient ON/OFF ganglion cell: G6. A: Vertically reconstructed camera-lucida drawing of G6, a small field, broadly bistratified ganglion cell with wavy, non-tapering dendrites. The amacrine cell layer (ACL) and ganglion cell layer (GCL) are indicated. The sublamina *a/b* border, at approximately L40 of the IPL (see text), appears to bisect the two dendritic strata. The horizontal line to the left denotes an approximate distance of 150 μm from the visual streak. The G6 axon is indicated with arrowheads. B: Physiological record of G6. First column: spot and annulus series with dim white flashes. A 0.21-mm spot (1) elicited spikes at onset and offset. With spot diameters of 0.67 mm (3) and 3.17 mm (9), spikes are suppressed, and the cell is somewhat hyperpolarized, indicative of a small receptive-field center and strong spatial opponency. Stimulated with a 0.92-mm i.d. annulus (12), G6 is clearly hyperpolarized. Columns 2–4: Responses to 0.21-mm flashes of red (694 nm), green (514 nm), and blue (450 nm) light at different attenuation levels with neutral density (ND) filters. With decreasing attenuation, red elicits increasingly sustained hyperpolarization, and decreasing transient depolarizations at onset and offset. Green elicits a sustained depolarization below apparent spike threshold (−2.5 ND) and pronounced ON and OFF transient depolarizations, accompanied by spikes at higher intensities (−1.5 N.D. and −0.5 N.D. attenuation). The response to blue with −0.5 ND appears qualitatively similar to the green response. Relative color intensities: log $q/\mu^2/500$ ms flash: −0.5 ND, −1.5 ND, −2.5 ND attenuated red (6.20, 5.07, 3.98); −0.5 ND, −1.5 ND, −2.5 ND attenuated green (5.42, 4.26, 3.16); −0.5 ND, −1.5 ND attenuated blue (4.72, 3.59).

Border regions of the amacrine cell layer and ganglion cell layer have been schematized in stipple (Fig. 3A). The cell had a compact dendritic arbor (140 μm $\times$ 120 μm), with wavy, highly branched, non-tapering dendrites. It was broadly bistratified, with its distal stratum clearly within sublamina *a* and its proximal stratum entirely within sublamina *b*. The peak densities of the distal and proximal dendritic strata were near L20-25 (S1/2) and L60 (S3/4), respectively, with branches spanning L10-85 (S1-4/5) of the IPL. The ellipsoidal soma had dimensions of 10 μm $\times$ 14 μm.

Among the Golgi-impregnated ganglion cells described by Kolb and co-workers from retinal wholemounts (Kolb, 1982; Kolb et al., 1988), G6 appears to be the closest morphological equivalent. Kolb et al. (1988) summarized the stratification of G6 (from the examples they had found in two related species) to be bistratified at S1/2 and S4. The dendritic morphology, arbor shape, and expanse of their illustrated examples of G6 show strong resemblance to the HRP-injected ganglion cell described herein.

Ultrastructure

In the retinal region where our G6 lay, the overall tissue preservation and contrast were good. Since a couple of Müller cells became labeled with HRP along with G6, their electron-dense profiles were sometimes found among the solidly filled G6 dendrites. The Müller cell processes were easily distinguished by their dense packing of glycogen and more diffuse HRP label. The central G6 dendrites were solidly electron-opaque (Figs. 4–7, asterisks), whereas the most peripheral dendrites were characterized by a less dense, granular and flocculent fill (Figs. 6 and 7A). Because the reaction product in some of the main arbor's profiles appeared to bleed into the cell membrane, obscuring the synaptic regions (Figs. 4 and 5), synaptic inputs to peripheral G6 dendrites were easier to read (Figs. 6 and 7A).

Clear examples of neurochemically labeled amacrine cell synapses, as well as (unlabeled) bipolar cell synapses, onto the dendritic arbor of G6 were surveyed. A partial reconstruction through approximately 10 μm of peripheral dendrites yielded 37 amacrine cell and three bipolar cell synapses onto G6, overall. Apparently, amacrine cells were the predominant input, particularly onto the G6 periphery. GABAergic and glycinergic amacrine cell synapses and bipolar cell synapses onto G6 are accounted for below. The reconstructed peripheral dendrites as well as surveyed regions of the main dendritic arbor of G6, that were not reconstructed, are included in the summary region (see Fig. 9).

GABAergic inputs to G6: autoradiography

The retina containing the HRP-injected G6 was incubated in [³H]-GABA plus nipecotic acid. As mentioned above, not all [³H]-GABA plus nipecotic acid incubated preparations gave optimal label distribution. This particular preparation was incubated as whole retina and the label density was probably not as high in the distal IPL, as compared to proximal regions. Nevertheless, the GABAergic label was quite specific and the ultrastructural autoradiographic data provide useful information about the circuitry of the proximal dendritic stratum of G6. Figure 4 presents a GABAergic synapse onto G6 near L85, the proximal extent of its arbor. This is one of three GABAergic synapses found in these preparations, onto the broad proximal stratum of G6. Since the GABAergic strata in the proximal IPL were heavily favored in this sample, clear autoradiographic ev-

Fig. 4. EM autoradiography: GABAergic input to G6 dendrite (asterisk) near L85 of the IPL, in sublamina *b*. Several vesicles are seen on the presynaptic membrane; the synapse is framed by arrowheads. M: indicates a nearby Müller cell process.
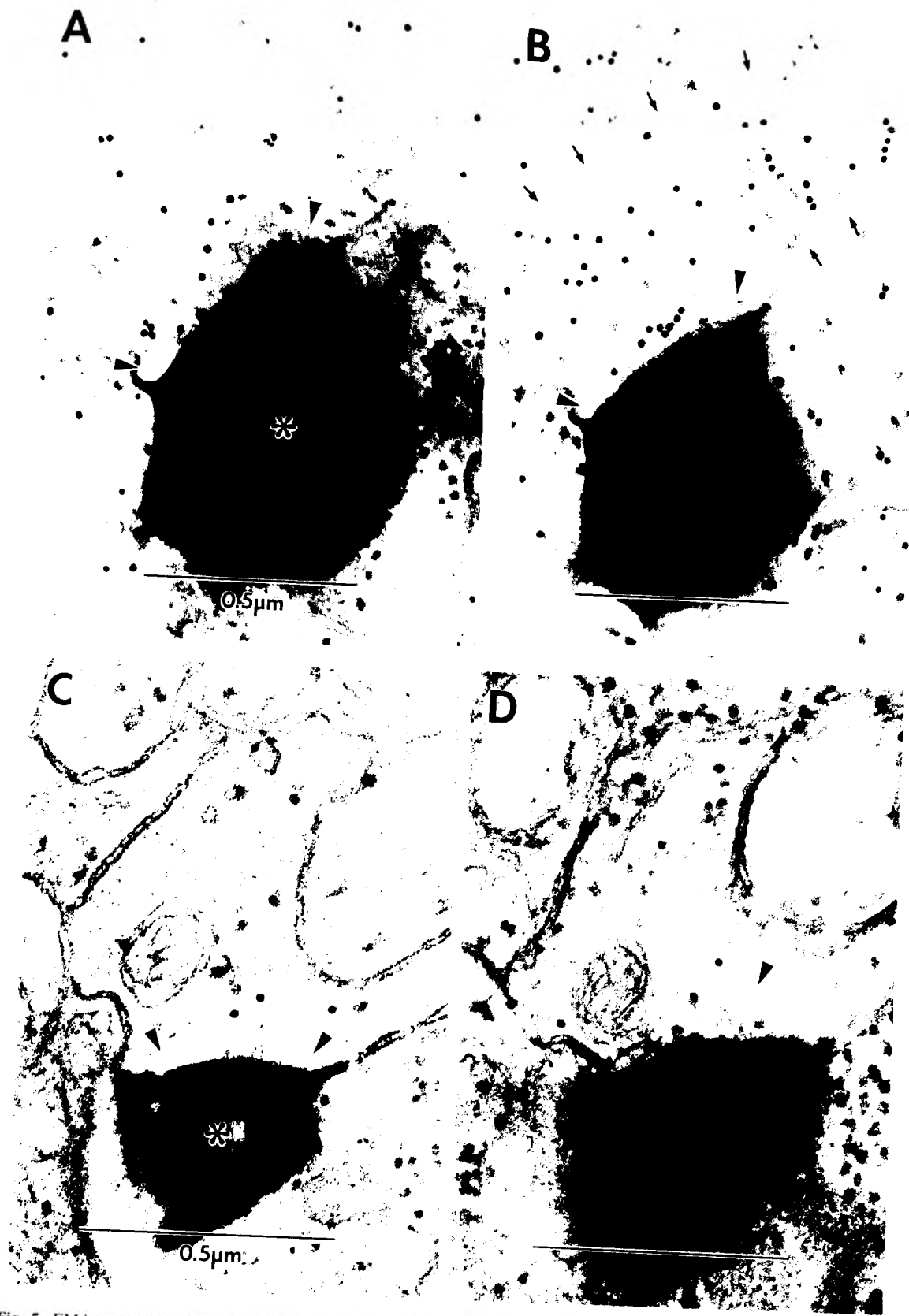
Fig. 5. EM immunocytochemistry: GABAergic inputs onto the distal dendritic stratum of G6 (sublamina *a*). Solid, very dense HRP reaction product in these profiles partially obscures synaptic morphology. A,B: Serial sections of GABAergic amacrine cell synapse near L40 of the IPL, onto a G6 dendrite (asterisk). Vesicles are clustered around a broad synaptic cleft (better oriented in A), framed by arrowheads. B: A more extended GABA-labeled amacrine cell profile, part of whose membrane is in grazing section (small arrows). C,D: Serial sections of GABAergic amacine cell synapse (arrowheads) onto G6 dendrite (asterisk) near L20-25 of the IPL.

0.5μm

0.5μm

0.5μm
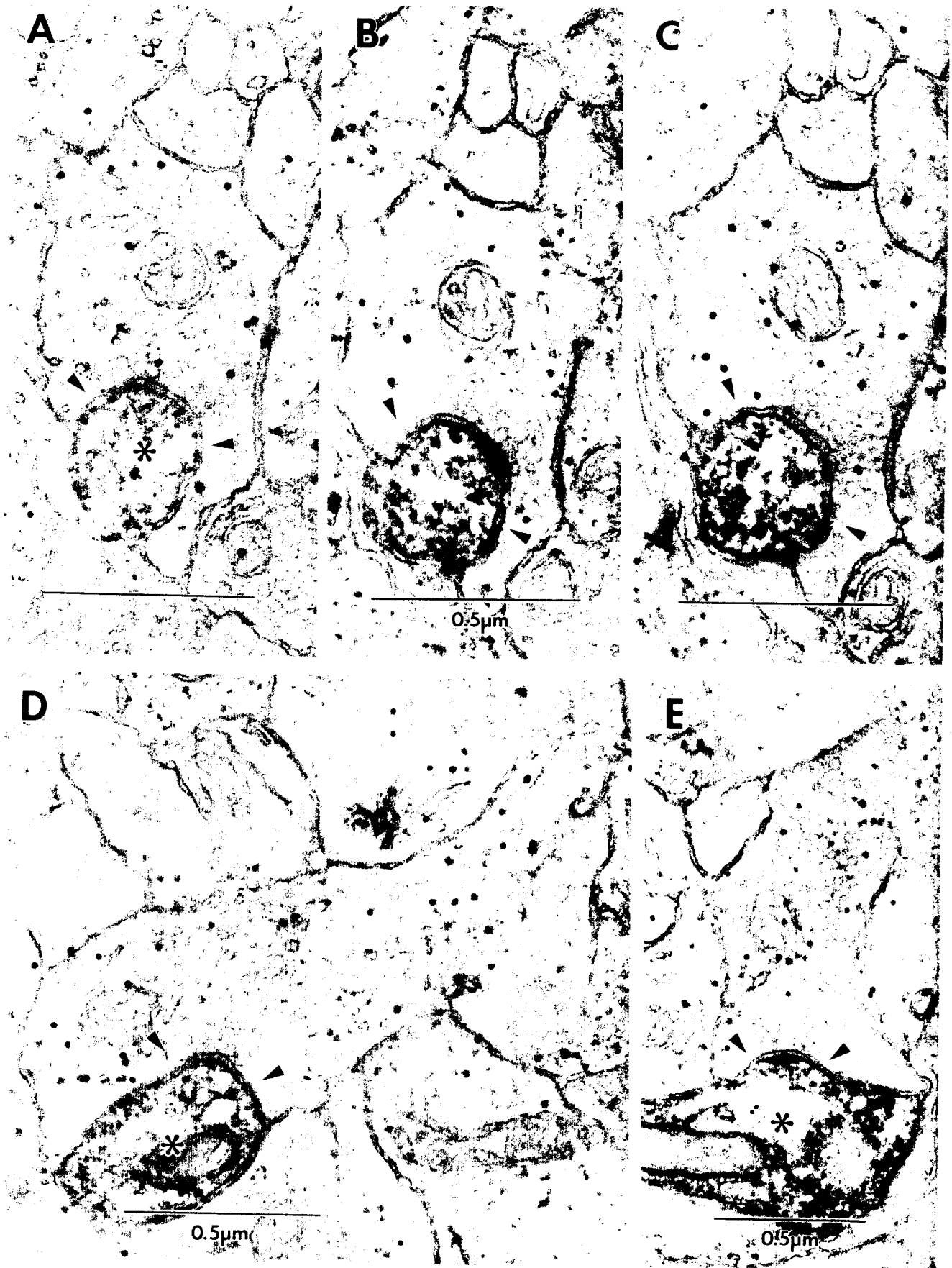
iden
ficu
data

GAF
IPL
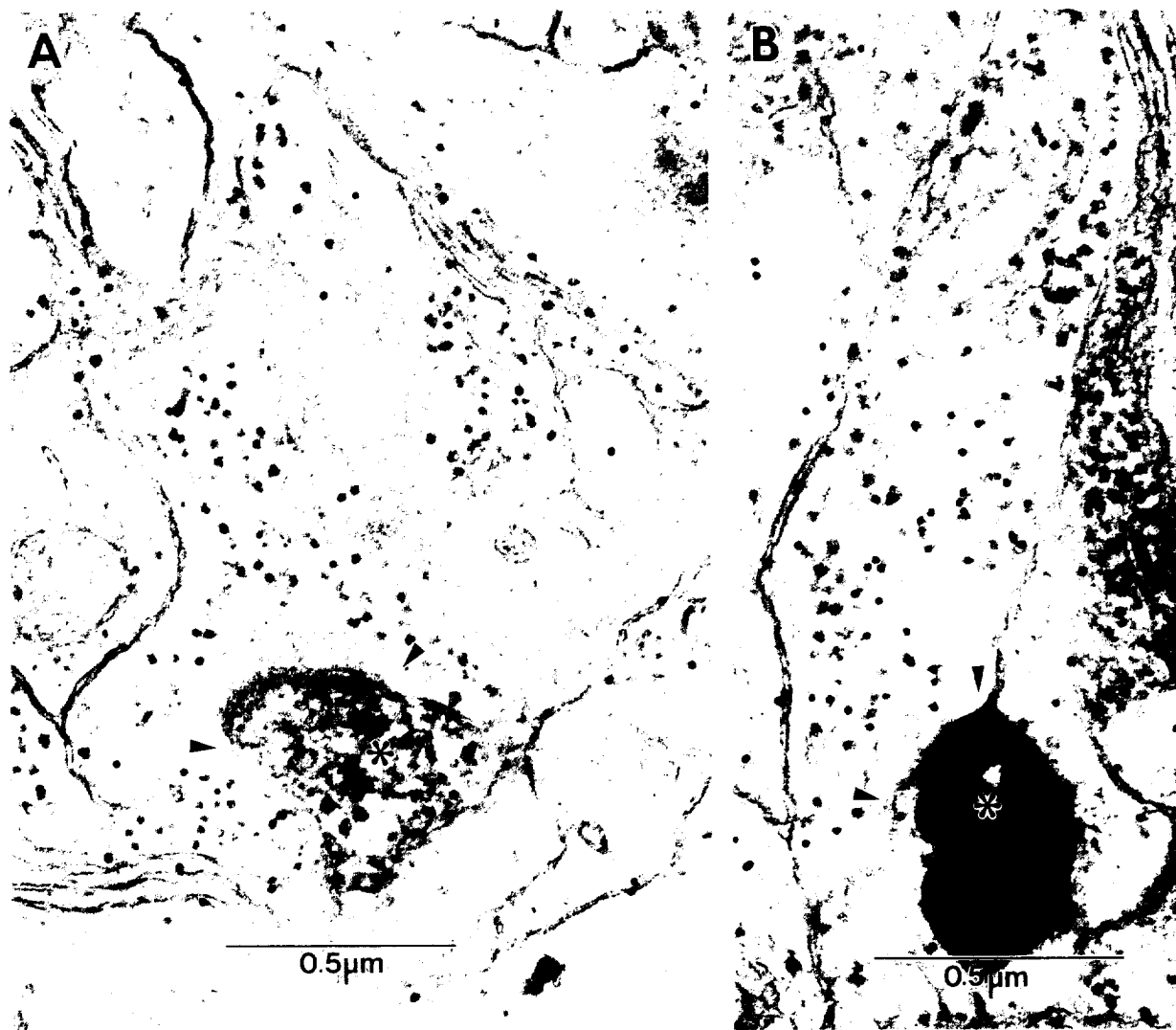
Fig. 7. EM immunocytochemistry: Glycinergic input to G6. A: Glycinergic amacrine cell synapse (arrowheads) onto G6 peripheral dendrite (asterisk) near L70 of the IPL. B: Glycinergic synapse onto G6 dendrite near L60 of the IPL. Gold particles are well-localized to a long, narrow amacrine cell profile.

idence of GABAergic input onto the distal arbor of G6 was difficult to find. The three synapses drawn from autoradiographic data are indicated as "*" in the schematic diagram of Fig. 9.

GABAergic inputs to G6: immunocytochemistry

Figure 5A, with a high gold particle density, presents a GABAergic synapse onto the main arbor of G6, near L40 of the IPL. This G6 profile shows evidence of the previously men-

tioned "bleeding" of the DAB reaction product into the synaptic cleft. Fortunately, the broad thickening of the synaptic cleft is apparent in Fig. 5A as is the vesicle aggregation; and there is clear gold localization to the presynaptic profile (Fig. 5B, small arrows). Figures 5C and 5D show two serial sections of a GABAergic input onto G6 near L20-25. Specificity of the immunocytochemical label was not as good as it was for autoradiography (see Methods), but by following each putatively

---

FACING PAGE

Fig. 6. EM immunocytochemistry: GABAergic inputs to peripheral dendrites of G6 (see Fig. 9, open circles). A-C: Serial sections of fairly large GABAergic synapse (arrowheads) onto a small G6 dendritic profile (asterisk), near L50 of the IPL. Dense, flocculent HRP reaction product leaves a clear view of the synaptic morphology. D: GABAergic synapse (arrowheads) onto G6 dendrite (asterisk) near L60-65 of the IPL. E: GABAergic synapse, near L50-55 of the IPL, onto a larger G6 profile, extending to the left of this view.

labeled synapse for at least three sections we were more confident of both consistency of label intensity and the presence of a synapse.

GABAergic synapses onto peripheral G6 dendrites are shown in Fig. 6 (arrowheads). Figures 6A–6C show three serial sections of a G6 dendrite at L50 of the IPL, Fig. 6D was near L60-65, and Fig. 6E was near L50-55. In these G6 dendrites, the characteristically dense, flocculent DAB reaction product (Muller & Marc, 1990) was easily recognizable and did not obscure the dendritic or synaptic morphology.

Figure 9 schematizes the major and minor dendritic strata of G6 according to the camera lucida drawing seen in Fig. 3A. Although G6 receives GABAergic input onto both its proximal and distal strata, GABAergic synapses appear to predominate proximally, between L50-75. The percent levels in the IPL where GABAergic inputs onto G6 occurred, as drawn from immunocytochemical data, are indicated with a "•" in the GABA column of Fig. 9.

Glycinergic inputs to G6: immunocytochemistry

We counted four clear examples of glycinergic input onto G6 dendrites from our immunocytochemical preparations. These synapses occurred between L50-70, on the proximal dendritic stratum of G6. Figure 7 presents examples from the peripheral (A) and main (B) arbors, near L70 and L60, respectively. The levels in the IPL where glycinergic inputs occurred are symbolized as "•" for synapses onto the main arbor, and "o" for input onto peripheral dendrites, in the GLYCINE column of Fig. 9.

Bipolar cell inputs

Bipolar cell synapses are found at all levels of the G6 dendritic arbor, from near L20-25 to L75, and are approximately evenly distributed between the proximal and distal strata. The three bipolar cell synapses we encountered in the peripheral ar-

bor were on the proximal stratum. Figure 8 presents examples of bipolar cell input (arrows) from the main and peripheral arbors, at L55 (Fig. 8A) and near L70-75 (Fig. 8B), respectively. In Fig. 9, bipolar cell inputs to the main arbor of G6 are symbolized as "▲" in the BIPOLAR column, and bipolar cell synapses onto peripheral dendrites are symbolized as "△."

ON-center ganglion cell (G10)

Physiological recordings

Two examples of morphologically similar ganglion cells, from two different preparations, gave characteristic sustained ON responses to dim white flashes (see Fig. 10A). In both cases, a 0.67-mm spot (spot 3) gave the clearest ON-center response; the response to a smaller spot was less distinctive. For both cells, a 0.92-mm-i.d. annulus (annulus 12) elicited a sustained hyperpolarization, indicating a spatially opponent surround. In neither case could we see evidence of color coding.

Morphology

Each cell was reconstructed from vertical sections with camera lucida (Figs. 10B and 10D). For one of these cells, we have a drawing from wholemount (Fig. 10C). In each case, the cell most resembled G10, which from previous studies of Golgi impregnation was seen to be bistratified to S3 and S5 (Kolb, 1982; Kolb et al., 1988). The HRP-injected examples described herein were predominantly bistratified, with primary dendrites that tapered, became wavy, and emitted fine wavy branches and had a dendritic expanse of about 200 μm. They were mainly bistratified at L58-70 (S3/4) and L85-100 (S5) of the IPL. One notable difference between the previous descriptions from Golgi-impregnated wholemounts (Kolb, 1982; Kolb et al., 1988) and our HRP-injected preparations is our finding of some dendritic branches near L40 (S2/3) in our present examples
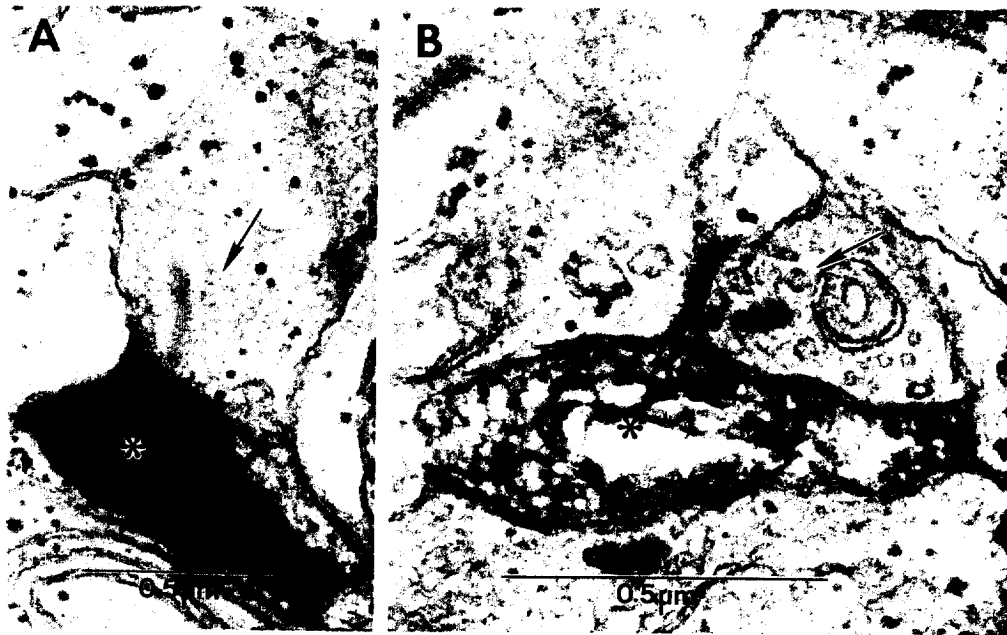
Fig. 8. A: Bipolar cell ribbon synapse (arrow) onto G6 dendrite (asterisk) near L55 of the IPL. B: Bipolar cell ribbon synapse (arrow) onto G6 peripheral dendrite, near L70-75 of the IPL.
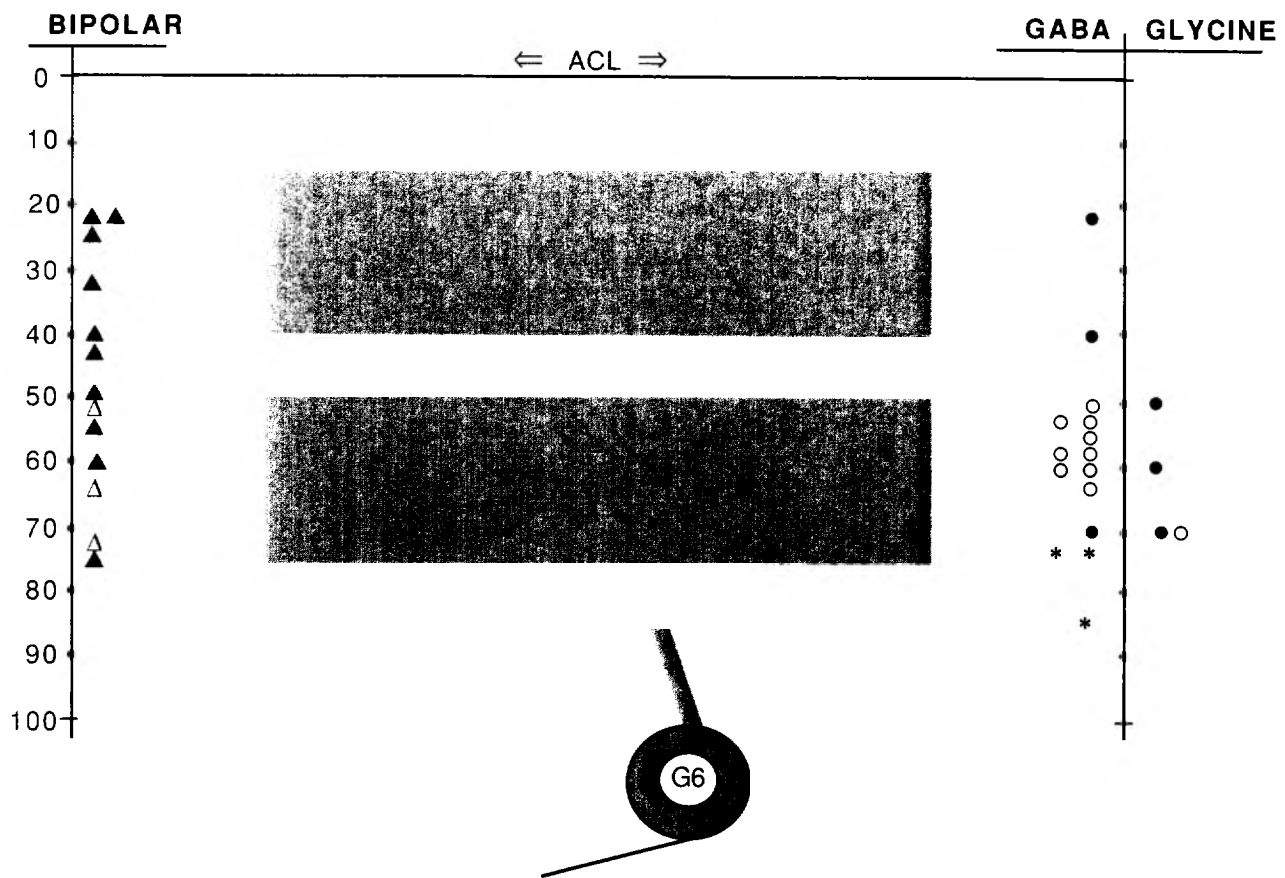
Fig. 9. Schematic summary diagram: synaptic inputs to G6. The schematic of G6 represents the major and minor dendritic strata (dark and light shaded areas) and their levels in the IPL. The two major strata fall near L15-40 in sublamina *a* and L50-75 in sublamina *b*; dendritic branches occur from L10-85. The columns to the left and right indicate the levels in the IPL where bipolar cell, GABAergic amacrine cell, and glycinergic amacrine cell synapses onto G6 occurred. Solid triangles (▲) symbolize bipolar cell synapses onto the main dendritic arbor of G6, while open triangles (△) indicate bipolar cell synapses onto the partially reconstructed peripheral G6 dendrites. Similarly, filled circles (●) symbolize immunocytochemically labeled synapses surveyed from the major portion of the G6 dendritic arbor; and open circles (○) indicate immunocytochemically labeled amacrine cell synapses onto the reconstructed peripheral dendrites. Asterisks (*) symbolize GABAergic inputs drawn from autoradiographic preparations (see Fig. 4, text). ⇐ACL⇒: amacrine cell layer.

(Figs. 10B and 10D). Even considering these projecting branches, the dendritic arbors of these HRP-labeled G10 ganglion cells were apparently restricted to sublamina *b*.

The physiological recordings (Fig. 10A) represent the cell pictured in Fig. 10B; the ultrastructure and cytochemistry presented in Figs. 11-14 are data from the cell pictured in Fig. 10D. A partial reconstruction of that dendritic arbor (Fig. 10D) revealed that the predominant input to G10 was from amacrine cells, with 55 amacrine cells and seven bipolar cells counted. The distributions of GABAergic and glycinergic amacrine cell synapses onto G10 are described below.

Glycinergic inputs onto G10: autoradiography

After physiological recording, the retina containing the HRP-injected G10 was incubated in [³H]-glycine. Autoradiographic evidence of glycinergic input onto G10 dendrites was found between L60-65 and L85-90 of the IPL. Figures 11A and 11B are examples of two serial sections from L75. The seven

glycinergic synapses found onto G10, drawn from high-affinity glycine uptake data, are represented in the schematic of Fig. 15, as "*" in the GLYCINE column. Their placement along the axis shows where each was stratified.

Glycinergic inputs to G10: immunocytochemistry

The immunocytochemical data for glycinergic synapses onto G10 dendrites are part of a partial reconstruction of the cell's dendritic tree. In these preparations, glycinergic synapses onto G10 were found mostly between L75-95, with one near L45-50. The reconstructed 40-μm vertical section was adjacent to the soma. Therefore, we can draw useful information about the distribution of such inputs onto central and peripheral dendrites. The approximate locations of these glycinergic synapses on the dendritic arbor are indicated in Fig. 15 (as "↓" on the schematized dendritic strata). The labeled synapse shown in two serial sections of Figs. 12A and 12B occurred on a peripheral dendrite of G10, near L95 of the IPL (see Fig. 15). The glycinergic am-
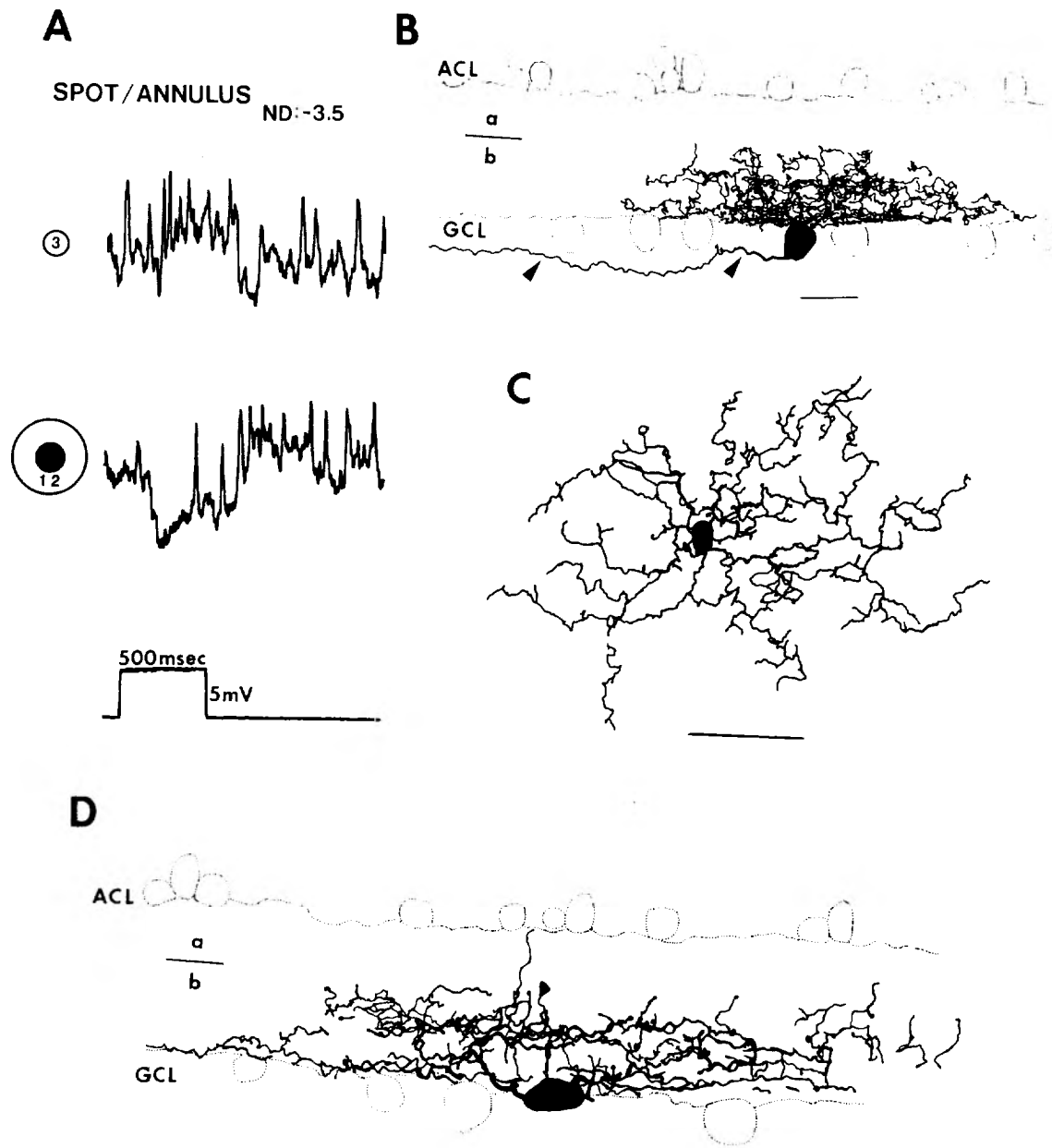
Fig. 10. ON-center ganglion cell: G10. A: Brief physiological record of one of two G10 ganglion cells studied. Stimulation with dim white 0.67-mm spot (3) elicited a sustained depolarization and increased spike rate. An annulus with 0.92-mm i.d. (12) elicited a sustained hyperpolarization, indicative of a spatially opponent surround. B,C: Camera-lucida drawings of the cell whose physiology is depicted in A. B: Vertical reconstruction, axon is indicated with arrowheads (scale bar = 20 μm). C: Camera-lucida drawing in wholemount (scale bar = 50 μm). D: Vertical reconstruction of a second G10 ganglion cell, whose synaptology was studied herein (scale bar = 20 μm). Both B and D show G10 to be bistratified in the proximal IPL (sublamina *b*). Approximate sublamina *a/b* borders are indicated.

acrine cell profile in Fig. 12A was not only presynaptic to G10, but to another profile as well (arrow), which was probably a non-glycinergic amacrine cell.

GABAergic inputs to G10: immunocytochemistry

GABAergic inputs onto G10 were found to costratify with many glycinergic inputs: most were within the L85-95+ levels of the IPL, with one each near L75-80 and L45-50. The GABAergic synapse (arrowheads) shown serially in Figs. 13A and 13B is on a peripheral dendrite, near L95. The schematic drawing in Fig. 15 shows the approximate locations of GABAergic synaptic inputs onto G10 (symbolized as " ⇓ " on the schematized dendritic strata, and indicated with " ● " in the GABA column).

Bipolar cell inputs

The bipolar cell synapses onto G10 appear equally divided between the two major dendritic strata (see Fig. 15). Five were found between L55 and L70-75 of the IPL, and six were found within L85-95+ (indicated as " ▲ " on the BIPOLAR column,
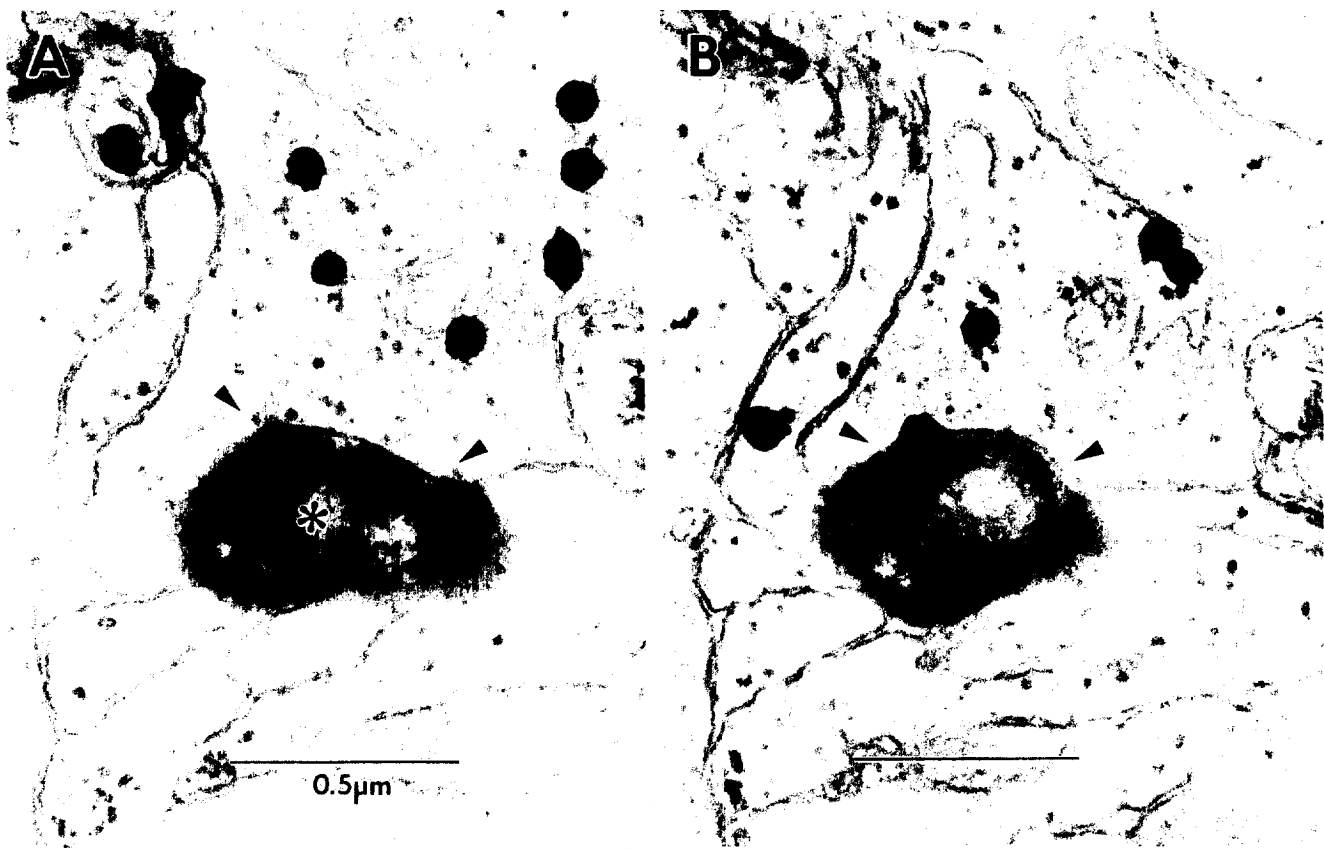
Fig. 11. A,B: Serial EM autoradiographs of glycinergic amacrine synapse (arrowheads) onto a G10 dendrite (asterisk) near L75-80 of the IPL, between the two major dendritic strata of G10. Silver grains are well-localized to the presynaptic profile.

Fig. 15). Inputs to the major distal stratum (approximately L55-70) appeared clustered near the soma, while synapses on the proximal dendrites (L85-95+) occurred further out on the periphery (symbolized as "▽" on the schematized dendritic strata, Fig. 15). The two electron micrographs show bipolar synapses at L85 (Fig. 14A) and L95 (Fig. 14B) of the IPL.

Discussion

In this paper, we have been able to describe the synaptology of two physiologically and morphologically distinct ganglion cells in the turtle retina. Intracellular recordings have characterized these two ganglion cell types as (1) a transient ON/OFF, color-opponent cell (G6) and (2) a sustained ON-center cell with a spatially opponent surround (G10). Electron microscopy of these two varieties of ganglion cell show that while both are dominated by amacrine cell synaptic input, significant bipolar cell input is present. The sustained cell appears to receive a greater proportion of bipolar cell input than the transient cell. EM autoradiography and immunocytochemistry for the inhibitory neurotransmitters GABA and glycine indicate that there are some significant differences in input for the two physiological types of cell. The transient ON/OFF, color-opponent cell receives relatively more GABAergic synapses than the sustained ON cell, and glycinergic input provides a relatively greater contribution to the sustained cell than to the transient cell. We shall discuss these differences in synaptic inputs and their likely relevance to the receptive-field architecture of these two ganglion cell types below.

ON/OFF color-opponent ganglion cell: G6

G6 is a broadly bistratified ganglion cell with dendrites fairly equally divided between sublamina *a* and sublamina *b* of the IPL. Its center response is transient ON/OFF with a sustained chromatic component that is hyperpolarizing to red and depolarizing to green. The surround response (to dim white flashes) shows spatial opponency. A sustained hyperpolarization emerges with increasing spot sizes and is clearly evoked by an annulus of relatively small inner diameter. However, our chromatic analysis of the surround was inconclusive so we cannot say, at present, whether the spatially opponent surround of G6 is color opponent.

As in all vertebrates studied, ON/OFF ganglion cells have been previously described in turtle (Lipetz & Hill, 1970; Bowling, 1980; Marchiafava & Weiler, 1980; Marchiafava & Wagner, 1981; Jensen & DeVoe, 1983; Marchiafava, 1983; Ariel & Adolph, 1985; Adolph, 1989; Granda & Fulbrook, 1989), as have color-opponent ganglion cells (Marchiafava & Wagner, 1981; Granda & Fulbrook, 1989). The latter ganglion cells have generally been described as sustained ON or sustained OFF to given wavelengths (Daw, 1968; Gouras, 1968; Marchiafava & Wagner, 1981; Granda & Fulbrook 1989). For example, Marchiafava and Wagner (1981) described sustained chromatic ganglion cells in turtle, whose center responses were red-OFF/
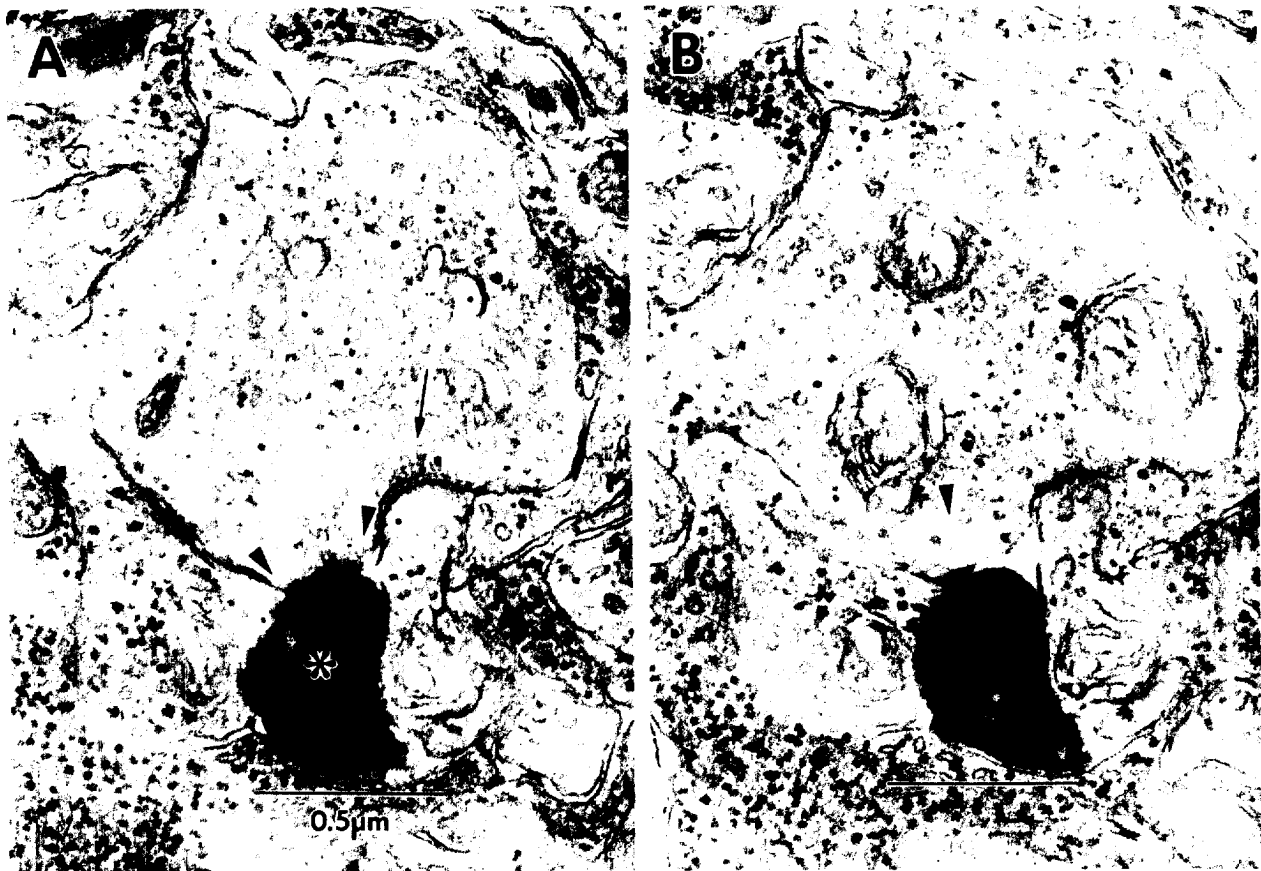
Fig. 12. A,B: Serial electron micrographs: Glycine-immunoreactive amacrine cell synapse (arrowheads) onto a G10 dendrite (asterisk) near L95, close to the proximal border of the IPL. The glycineric amacrine cell profile is also presynaptic to another process (arrow in A), probably an unlabeled amacrine cell.
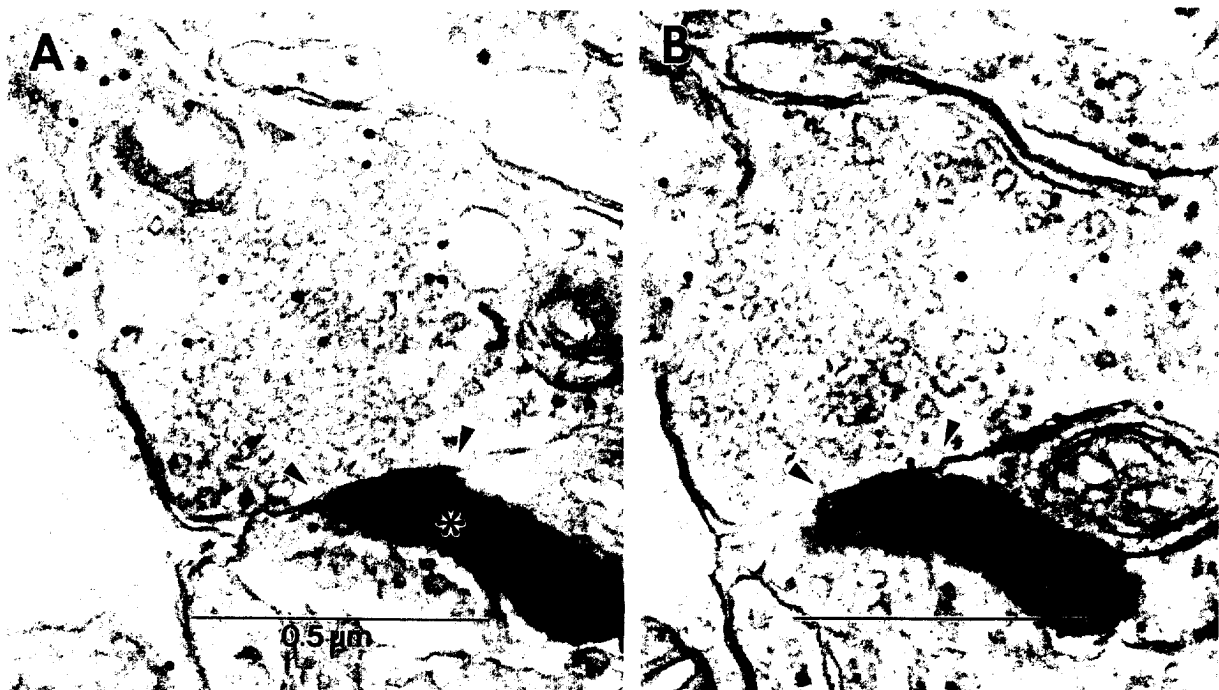
Fig. 13. A,B: Serial electron micrographs: GABA-immunoreactive vesicle-filled amacrine cell profile, synapsing onto G10 dendrite (asterisk) near L95 of the IPL. Arrowheads frame the synapse.
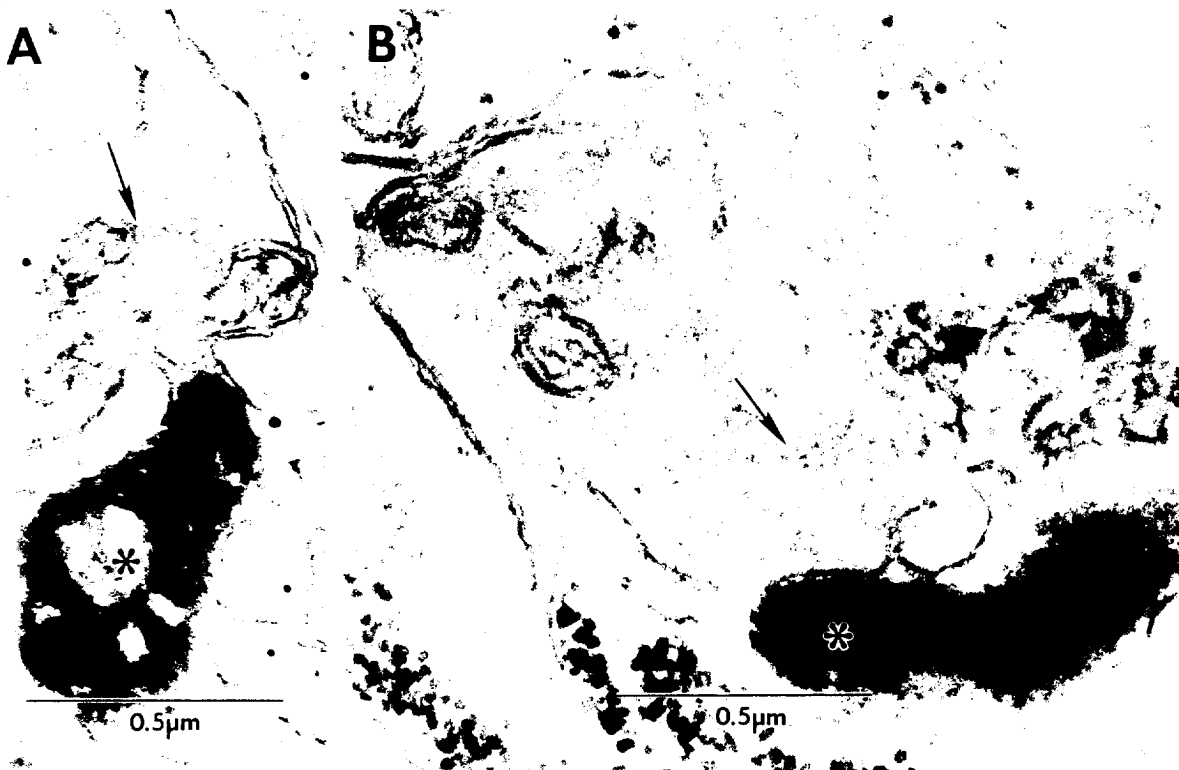
Fig. 14. A,B: Bipolar cell ribbon synapses (arrows) onto G10 dendrites (asterisks) near L85 (A) and L95 (B) of the IPL, respectively.
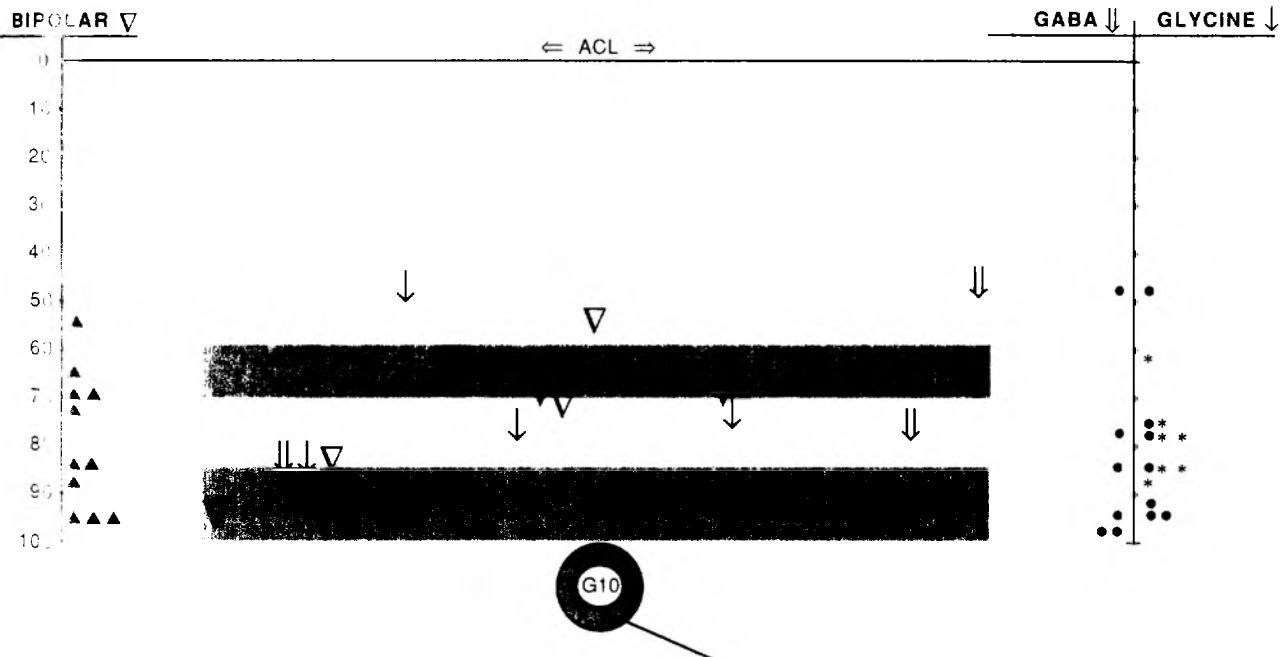
Fig. 15. Schematic summary diagram: synaptic inputs to G10. The schematic of G10 depicts the major and minor strata of G10 and their levels in the IPL, based on vertical reconstructions (see Fig. 10). The two major dendritic strata lie near L60-70 and L85-100 of the IPL. Branches exist between the strata, and distally up to near L40, close to the sublamina *a/b* border. The dendrites of G10 are within sublamina *b*. The columns to the left and right of the G10 schematic show the stratification of bipolar cell (▲), GABAergic amacrine cell and glycinergic amacrine cell synapses, drawn from immunocytochemical (●) and autoradiographic preparations (*). Immunocytochemical preparations were partially reconstructed so that the locations on the G10 dendritic arbor of bipolar cell (▽), GABAergic amacrine cell (⇊), and glycinergic amacrine cell synapses (↓) could be represented (see text). ⇐ACL⇒: amacrine cell layer.

green-ON; some of their surrounds were only spatially opponent, while others were chromatically opponent. Therefore, the sustained red-OFF/ green-ON components of the G6 receptive-field center response have been described in other turtle ganglion cells. Also, the possibly achromatic, spatially opponent surround that our data on G6 suggest is not unprecedented. However, a *transient* ON/OFF ganglion cell that is *color opponent*, such as G6, has not been previously reported. Another G6, with similar physiological and morphological properties as the one described herein has recently been found (Ammermüller, unpublished observations), but its synaptology has not been analyzed by electron microscopy as yet.

Figure 9 schematizes the stratification of GABAergic, glycinergic, and bipolar cell inputs to G6 as described in this study. From autoradiographic preparations, we found a few GABAergic synapses onto the proximal dendrites of G6. Immunocytochemical analysis gave us more information on the density and distribution of the GABAergic synapses, as well as defining the glycinergic input to G6. GABAergic and glycinergic synapses costratified on the proximal dendritic stratum, between L50-70 of the IPL (sublamina *b*) while GABAergic inputs were found in addition at two levels of the distal stratum of G6, near L20-25 and L40 (sublamina *a*).

A partial reconstruction was done of the peripheral dendritic arbor of G6, of which approximately 10 μm of cross-sectional depth met our criteria for immunocytochemical analysis. The dendrites sampled in this series were between L40-75 of the IPL, mostly in the proximal stratum of G6. In the series analyzed for GABAergic input, nine of 23 (39%) of the amacrine cell synapses onto G6 dendrites were clearly GABAergic. In the glycine-immunoreactive samples, only one of 14 (7%) of the amacrine cell synapses onto G6 was clearly glycinergic (see Fig. 9, open circles). Given the stringency of our criteria, both of these proportions are probably underestimates. In any event it appears, at least on peripheral dendrites of G6, that GABAergic amacrine cell inputs are predominant.

In the partial reconstruction of the G6 peripheral arbor described above (Fig. 9, open symbols), of the 40 synaptic inputs counted onto G6, three were from bipolar cells (7.5%). By comparison, Guiloff et al. (1988) estimated 8.6% of the synapses onto putative turtle ganglion cell profiles from bipolar cells. Marshak et al. (1988) retrogradely labeled goldfish ganglion cells with HRP and found, through ultrastructural analysis, that their dendrites received 6% of their inputs from bipolar cells. Therefore, our estimated proportion of bipolar cell inputs to G6 peripheral dendrites is not unusual, given previous findings. Overall, bipolar cell synapses onto G6 were found at all levels of the G6 dendritic arbor. They occurred between L20-25 and L75 of the IPL and were approximately evenly distributed between the distal and proximal dendritic strata (see Fig. 9): six were found onto the distal stratum (sublamina *a*) and seven occurred onto the proximal stratum (sublamina *b*). Sensory cells with ribbon synapses, such as photoreceptors and bipolar cells, have been associated with extraordinary sensitivity and high gain (Fain, 1977; Koch et al., 1986). Therefore, even a relatively low percentage of bipolar cell inputs can have great impact on a ganglion cell's response properties.

An important question is, what neuronal inputs are likely to provide the receptive-field properties of G6? Based on studies using low chloride blockade of the ON-center pathway (Miller & Dacheux, 1976; Miller, 1979), and pharmacological blockade by glutamate analogs, of either ON or OFF pathways

(Slaughter & Miller, 1981, 1983*a,b*; Miller & Slaughter, 1986; Massey & Miller, 1988), it has been demonstrated that transient ON/OFF ganglion cells receive input from both ON- and OFF-center bipolar cells. Intracellular recordings from turtle bipolar cells indicate that a number of them have color-opponent center responses with non-color opponent surrounds (Yazulla, 1976). However, all of the color-opponent bipolar cells so far described have been red-ON/green-OFF-center bipolar cells (with either an ON or OFF surround to all wavelengths). We suppose that it is quite likely that red-OFF/green-ON-center bipolar cells, as required for input to our G6 cell, could be present in turtle as well. Thus a red-OFF/green-ON-center bipolar cell with an OFF surround could supply the chromatic components of the G6 center response, and would be consistent with our data about its surround.

Bipolar cells B4 and B8 (Kolb, 1982) are good candidates for OFF-bipolar cell inputs to G6; their terminal stratifications correspond to the IPL levels of bipolar cell synapses onto the G6 distal dendritic stratum (see Fig. 9). Similarly, B6 and B7 (Kolb, 1982) are good candidates for ON-bipolar cell input to G6. It is difficult to speculate which bipolar cell types could contribute chromatic information, since there is no correlative morphology for the previously described color-opponent bipolar cells (Yazulla, 1976). Multistratified bipolar cells B3 and B7 (Kolb, 1982) are both possibilities.

Alternatively to bipolar cell input, a small-field color-opponent amacrine cell could contribute to the G6 ganglion cell's center response. Sustained or transient ON/OFF amacrine cells would gain color opponency by way of sign-conserving input from a red-ON/green-OFF bipolar cell, as described by Yazulla (1976). In fact, we have recorded, in turtle, from a sustained red-ON/green-OFF amacrine cell with a color-opponent surround (Muller et al., 1989) qualitatively similar to the transient and sustained color-opponent amacrine cells of fish (Djamgoz & Ruddock, 1983; Watanabe & Murakami, 1985; Djamgoz et al., 1990). Either amacrine cell type's sign-inverting input to G6 could give rise to its sustained red-OFF/green-ON response. Transient hyperpolarizations after stimulus onset and offset would serve as particular evidence for transient ON/OFF amacrine cell input (Miller & Dacheux, 1976; Miller, 1979; Frumkes et al., 1981). However, our results are not clear in that regard (Fig. 3B).

In summary, the transient ON/OFF responses of G6 are probably derived from ON- and OFF-bipolar cell input, while color-coded bipolar cells are likely to give rise to the sustained chromatic opponency of G6, either directly or through an intervening (and thus color-coded) amacrine cell. Since bipolar cell inputs were found distributed to many levels on both strata of the G6 dendritic arbor (see Fig. 9), ON-center, OFF-center, as well as color-coded bipolar cells could conceivably be participating. Sustained opponent surround properties of G6 could be provided by either GABAergic or glycinergic amacrine cell inputs, as both neurochemical systems are known to have sustained amacrine cell populations (Frumkes et al., 1981; Kolb & Nelson, 1985). However, our analysis of G6 inputs indicate that GABAergic amacrine cell inputs predominate.

ON-center ganglion cell: G10

In this report, two examples of ganglion cell G10 are presented. Both physiological recordings revealed a sustained ON-center response with a spatially opponent (sustained-OFF) surround,

with no discernable color opponency. Each example was broadly bistratified within sublamina *b*, with major dendritic strata near L60-70 and L85-100 of the IPL. The two physiological records for G10, although limited, correspondingly showed these cells to have relatively simple, concentric receptive fields. However, synaptic inputs to G10, as determined by ultrastructure and cytochemistry, appear to reflect greater complexity.

A partial reconstruction of G10, including all levels of its dendritic arbor, yielded 62 synaptic inputs of which seven were from bipolar cells (11.5%). As mentioned above, previous estimates in turtle (Guiloff et al., 1988) and goldfish retinas (Marshak et al., 1988) for the proportion of bipolar cell inputs onto ganglion cells were 8.6% and 6%, respectively. Therefore, our findings for G10 suggest a greater-than-average amount of bipolar cell input to this cell.

EM-autoradiographic and partially reconstructed EM-immunocytochemical data suggest multiple classes of GABAergic and glycinergic amacrine cells, and bipolar cells synapse onto G10 dendrites. Our partially reconstructed glycine-immunoreactive series revealed that of the 28 amacrine cell synapses onto G10, seven were clearly glycinergic (25%). The GABA-immunoreactive series yielded six of 17 amacrine cell inputs well-labeled for GABA (35%). As mentioned above, given our stringent criteria for labeled profiles, both of these proportions are probably underestimates. As depicted in Fig. 15, the seven additional glycinergic inputs drawn from autoradiographic preparations introduce a sample bias toward glycine. These data are useful, however; they give us a better view of the stratification of glycinergic input to G10. Regardless, GABAergic and glycinergic synapses onto G10 are both prevalent, but in comparison with G6, G10 clearly receives a higher proportion of glycinergic amacrine cell input.

The stratification of glycinergic and GABAergic synapses onto G10 dendrites shows a fair amount of overlap, particularly between L85-95+, in the proximal IPL. There were also examples of both GABAergic and glycinergic input onto the most distal branches of G10, near L45-50 (see Fig. 15). In addition, glycinergic synapses were prevalent between the major strata of G10: L75-80 (five of 14), while GABAergic synapses were not (one of six). Perhaps most notably, the GABAergic synapses appeared to be confined to the more peripheral dendrites of G10, while glycinergic synapses were distributed throughout the arbor (Fig. 15). This may connote a spatial division of labor, whereby GABAergic amacrine cells may specifically influence the outer surround of G10.

The distribution of neurochemical inputs onto G10 is consistent with inhibition by multiple populations of glycinergic and GABAergic sustained-ON amacrine cells. This is conceivable, as morphological evidence of distinct subtypes of glycinergic and GABAergic sustained-ON and sustained-OFF amacrine cells have been found in a number of other species (Kolb & Nelson, 1985; Maguire et al., 1989; Muller & Marc, 1990). The variety of glycinergic and GABAergic sustained amacrine cell inputs to G10 may contribute complex spatial properties to its opponent surround.

Bipolar cell inputs to G10 were not only evenly divided between the two major strata, but they appeared divided between the more central and peripheral arbors. The bipolar cell synapses onto the distal dendritic stratum ($\approx$L55-70+) of G10 were closer to the soma, whereas the bipolar cell inputs to the proximal dendritic stratum (L85-95+) were more peripherally located on the dendrites. It is likely that all bipolar cells that

synapse onto G10 are center-depolarizing (ON) contributing to the sustained ON-center response. One bipolar cell that could account for most of the inputs to G10 is B7 (Kolb, 1982), tristratified to L55, L70-75, and L85-90. However, all four candidates from those described by Kolb, likely to be ON-center bipolar cells, have terminals in S5: B1, B2, B6, and B7. Therefore, it is not clear which cells have the most proximal terminations, although B2 appears to terminate near L95 of the IPL. Considering that the six bipolar cell synapses that we found onto the proximal stratum of G10 were evenly divided between L95+ and L85-90, this is an important consideration. Regardless, it appears, by the stratification and distribution of their inputs, that more than one type of ON-bipolar cell contributes to the G10 receptive field.

One difference that we can predict between the bipolar cells with the more distal dendritic inputs to G10, that are nearer the soma, and the bipolar cells whose synapses are to the more proximal and peripheral dendrites, is their distinct circuitry. Since they end at different levels of the IPL, they should each receive a different complement of interneuronal input, which means that at the very least, their respective contributions to the surround would be unique. Could the peripherally located bipolar cell input be more responsible for the surround of the receptive field, whereas the central inputs are concerned with the receptive-field center?

General comments

Based on our results and previous work (Guiloff et al., 1988), we can predict that a high percentage of inputs onto turtle ganglion cells are from amacrine cells. A variety of turtle amacrine cells have been characterized both morphologically and physiologically (Ammermüller & Weiler, 1988, 1989; Kolb et al., 1988; Muller et al., 1989). Virtually all ganglion cells probably receive either GABAergic or glycinergic amacrine cell input, and most, if not all, receive both, although in different proportions as demonstrated in this paper. Marchiafava and co-investigators (Marchiafava & Weiler, 1980; Marchiafava & Wagner, 1981; Marchiafava, 1983) previously described "type A" ganglion cells as those whose receptive fields are determined by bipolar cells. However, we now understand that while the basic center-surround structure of ganglion cell receptive fields may be laid down in the outer retina, all ganglion cells are significantly influenced by amacrine cells. As we further study the finer points of ganglion cell receptive-field structure, the division of labor between bipolar and amacrine cell input will become clearer. Further physiological work using pharmacological blockers for GABA and glycine, as well as correlative cytochemical labeling, will help us dissect ganglion cell receptive fields neurochemically. We will then better understand the unique roles that GABAergic and glycinergic neurons play in how various ganglion cells function.

References

ADOLPH, A.R. (1989). Pharmacological actions of peptides and indole-amines on turtle retinal ganglion cells. *Visual Neuroscience* 3, 411–423.

AMMERMÜLLER, J. & WEILER, R. (1988). Physiological and morphological characterization of OFF-center amacrine cells in the turtle retina. *Journal of Comparative Neurology* 273, 137–148.

AMMERMÜLLER, J. & WEILER, R. (1989). Correlation between electrophysiological responses and morphological classes of turtle retinal amacrine cells. In *Neurobiology of the Inner Retina*, ed. WEILER, R. & OSBORNE, N., pp. 117–132. Berlin: Springer-Verlag.

ARIEL, M. & ADOLPH, A.R. (1985). Neurotransmitter inputs to directionally sensitive turtle retinal ganglion cells. *Journal of Neurophysiology* 54, 1123–1143.

BOUTEILLE, M. (1976). The "LIGOP" method for routine ultrastructural autoradiography: a combination of single grid coating, gold latensification, and phenidon development. *Journal de Microscopie et de Biologie Celluaire* 27, 121–128.

BOWLING, D.B. (1980). Light responses of ganglion cells in the retina of the turtle. *Journal of Physiology* 299, 173–196.

DAW, N.W. (1968). Colour-coded ganglion cells in the goldfish retina: extension of their receptive fields by way of new stimuli. *Journal of Physiology* 197, 567–592.

DJAMGOZ, M.B.A. & RUDDOCK, K.H. (1983). Spectral characteristics of transient amacrine cells in a cyprinid fish (roach) retina *in vitro*. *Journal of Physiology* (London) 339, 19P.

DJAMGOZ, M.B.A., SPADAVECCHIA, L., USAI, C. & VALLERGA, S. (1990). Variability of light-evoked response pattern and morphological characterization of amacrine cells in goldfish retina. *Journal of Comparative Neurology* 301, 171–190.

ELDRED, W.D. & CHEUNG, K. (1989). Immunocytochemical localization of glycine in the retina of the turtle (*Pseudemys scripta*). *Visual Neuroscience* 2, 331–338.

ELDRED, W.D. & KARTEN, H.J. (1983). Characterization and quantification of peptidergic amacrine cells in the turtle retina: enkephalin, neurotensin and glucagon. *Journal of Comparative Neurology* 221, 371–381.

FAIN, G.L. (1977). The threshold signal of photoreceptors. In *Vertebrate Photoreceptors*, ed. BARLOW, H.B., pp. 305–323. London: Academic.

FAMIGLIETTI, E.V., JR., KANEKO, A. & TACHIBANA, M. (1977). Neuronal architecture of on and off pathways to ganglion cells of the carp retina. *Science* 198, 1267–1269.

FRUMKES, T.E., MILLER, R.F., SLAUGHTER, M. & DACHEUX, R.F. (1981). Physiological and pharmacological basis of GABA and glycine action on neurons of the mudpuppy retina. III. Amacrine-mediated inhibitory influences on ganglion cell receptive field organization: a model. *Journal of Neurophysiology* 45, 783–805.

GOURAS, P. (1968). Identification of cone mechanisms in monkey ganglion cells. *Journal of Physiology* 199, 533–547.

GRANDA, A.M. & FULBROOK, J.E. (1989). Classification of turtle retinal ganglion cells. *Journal of Neurophysiology* 62, 723–737.

GUILOFF, G.D., JONES, J. & KOLB, H. (1988). Organization of the inner plexiform layer of the turtle retina: an electron microscopic study. *Journal of Comparative Neurology* 272, 280–292.

HARE, W.A., LOWE, J.S. & OWEN, G. (1986). Morphology of physiologically identified bipolar cells in the retina of the tiger salamander, *Ambystoma tigrinum*. *Journal of Comparative Neurology* 252, 130–138.

HENDRICKSON, A.E., KOONTZ, M.A., POURCHO, R.G., SARTHY, P.V. & GOEBEL, D.J. (1988). Localization of glycine-containing neurons in the *Macaca* monkey retina. *Journal of Comparative Neurology* 273, 473–487.

HURD, L.D., II & ELDRED, W.D. (1989). Localization of GABA- and GAD-like immunoreactivity in the turtle retina. *Visual Neuroscience* 3, 9–20.

JENSEN, R.J. & DEVOE, R.D. (1982). Ganglion cells and (dye-coupled) amacrine cells in the turtle retina that have possible synaptic connection. *Brain Research* 240, 146–150.

JENSEN, R.J. & DEVOE, R.D. (1983). Comparisons of directionally selective with other ganglion cells of the turtle retina: intracellular recording and staining. *Journal of Comparative Neurology* 217, 271–287.

KELLY, J.S. & WEITSCH-DICK, F. (1978). Critical evaluation of the use of radioautography as a tool in the localization of amino acids in the mammalian nervous system. In *Amino Acids as Chemical Transmitters*, ed. FONNUM, F., pp. 102–121. New York: Plenum.

KLEINSCHMIDT, J. & YAZULLA, S. (1984). Uptake of ^{3}H-glycine in the outer plexiform layer of the toad (*Bufo marinus*). *Journal of Comparative Neurology* 230, 352–360.

KOCH, C., POGGIO, T. & TORRE, V. (1986). Computations in the vertebrate retina: gain enhancements, differentiation, and motion discrimination. *Trends in Neuroscience* 9, 204–210.

KOLB, H. (1982). The morphology of the bipolar cells, amacrine cells, and ganglion cells in the retina of the turtle *Pseudemys scripta elegans*. *Philosophical Transactions of the Royal Society B* (London) 298, 355–393.

KOLB, H. & NELSON, R. (1985). Functional neurocircuitry of amacrine cells in the cat retina. In *Neurocircuitry of the Retina: A Cajal Memorial*, ed. GALLEGO, A., pp. 215–232. New York: Elsevier.

KOLB, H., PERLMAN, I. & NORMANN, R.A. (1988). Neural organization of the retina of the turtle *Mauremys capsica*: a light-microscope and Golgi study. *Visual Neuroscience* 1, 47–72.

KOLB, H.K., WANG, H.H. & JONES, J. (1986). Cone synapses with Golgi-stained bipolar cells that are morphologically similar to a center-hyperpolarizing and a center-depolarizing bipolar cell type in the turtle retina. *Journal of Comparative Neurology* 250, 510–520.

LIPETZ, L.E. & HILL, R.M. (1970). Discrimination characteristics of the turtle's retinal ganglion cells. *Experientia* 26, 373–374.

MAGUIRE, G., LUKASIEWICZ, P., WU, S. & WERBLIN, F. (1989). Physiological characterization of biochemically and morphologically identified sustained amacrine cells in the tiger salamander retina. *Investigative Ophthalmology and Visual Science* (Suppl.) 30, 62.

MARC, R.E. (1985). The role of glycine in retinal circuitry. In *Retinal Neurotransmitters and Modulators: Models for the Brain Vol. 2*, ed. MORGAN, W.W., pp. 119–158. Boca Raton, Florida: CRC Press.

MARC, R.E. (1986). Neurochemical stratification of the inner plexiform layer of the vertebrate retina. *Vision Research* 26, 223–238.

MARC, R.E. (1989). The anatomy of multiple GABAergic and glycinergic pathways in the inner plexiform layer of the goldfish retina. In *The Neurobiology of the Inner Retina*, ed. WEILER, R. & OSBORNE, N., pp. 53–64. Berlin: Springer-Verlag.

MARC, R.E. & LAM, D.M.K. (1981). Glycinergic pathways in the goldfish retina. *Journal of Neuroscience* 1, 152–165.

MARC, R.E. & LIU, W.-L. (1985). (^{3}H) Glycine-accumulating neurons of the human retina. *Journal of Comparative Neurology* 232, 241–260.

MARC, R.E., STELL, W.K., BOK, D. & LAM, D.M.K. (1978). GABAergic pathways in the goldfish retina. *Journal of Comparative Neurology* 182, 221–246.

MARCHIAFAVA, P.L. (1983). The organization of inputs establishes two functional and morphologically identifiable classes of ganglion cells in the retina of the turtle. *Vision Research* 23, 325–338.

MARCHIAFAVA, P.L. & WAGNER, H.G. (1981). Interactions leading to color opponency in ganglion cells of the turtle retina. *Proceedings of the Royal Society B* (London) 211, 261–267.

MARCHIAFAVA, P.L. & WEILER, R. (1980). Intracellular analysis and structural correlates of the organization of inputs to ganglion cells in the retina of the turtle. *Proceedings of the Royal Society B* (London) 208, 103–113.

MARIANI, A.P. & CASERTA, M.T. (1986). Electron microscopy of glutamate decarboxylase (GAD) immunoreactivity in the inner plexiform layer of the rhesus monkey retina. *Journal of Neurocytology* 15, 645–655.

MARSHAK, D., ARIEL, M. & BROWN, E. (1988). Distribution of synaptic inputs onto goldfish retinal ganglion cell dendrites. *Experimental Eye Research* 46, 965–978.

MASSEY, S.C. & MILLER, R.F. (1988). Glutamate receptors of ganglion cells in the rabbit retina: evidence for glutamate as a bipolar cell transmitter. *Journal of Physiology* 405, 635–655.

MILLER, R.F. (1979). The neuronal basis of ganglion cell receptive field organization and the physiology of amacrine cells. In *The Neurosciences Fourth Study Program*, ed. SCHMITT, F.O., pp. 227–245. Cambridge, Massachusetts: MIT Press.

MILLER, R.F. & DACHEUX, R.F. (1976). Synaptic organization and ionic basis of on and off channels in mudpuppy retina. III. A model of ganglion cell receptive field organization based on chloride-free experiments. *Journal of General Physiology* 67, 679–690.

MILLER, R.F. & SLAUGHTER, M.M. (1986). Excitatory amino acid receptors of the retina: diversity of subtypes and conductive mechanisms. *Trends in Neuroscience* 9, 211–213.

Mosinger, J.L., Yazulla, S. & Studholme, K.M. (1986). GABA-like immunoreactivity in the vertebrate retina: a species comparison. *Experimental Eye Research* 42, 631–644.

Muller, J.F. & Marc, R.E. (1984). Three distinct morphological classes of receptors in fish olfactory organs. *Journal of Comparative Neurology* 222, 482–495.

Muller, J.F. & Marc, R.E. (1990). GABAergic and glycinergic pathways in the inner plexiform layer of the goldfish retina. *Journal of Comparative Neurology* 291, 281–304.

Muller, J.F., Ammermüller, J., Kolb, H. & Normann, R.A. (1989). Physiological, anatomical and neurochemical studies on turtle amacrine and ganglion cells. *Investigative Ophthalmology and Visual Science* (Suppl.) 30, 122.

Nelson, R., Famiglietti, E.V., Jr. & Kolb, H. (1978). Intracellular staining reveals different levels of stratification for on- and off-center ganglion cells in cat retina. *Journal of Neurophysiology* 41, 472–483.

Pourcho, R.G. & Goebel, D.J. (1987). Visualization of endogenous glycine in cat retina: an immunocytochemical study with Fab fragments. *Journal of Neuroscience* 7, 1189–1197.

Pourcho, R.G. & Owczarzak, M.T. (1989). Distribution of GABA immunoreactivity in the cat retina: a light and electron microscopic study. *Visual Neuroscience* 2, 425–435.

Slaughter, M.M. & Miller, R.F. (1981). 2-Amino-4-phosphonobutyric acid: a new pharmacological tool for retina research. *Science* 211, 182–184.

Slaughter, M.M. & Miller, R.F. (1983a). An excitatory amino-acid antagonist blocks cone input to sign-conserving second-order retinal neurons. *Science* 219, 1230–1232.

Slaughter, M.M. & Miller, R.F. (1983b). Bipolar cells in the mudpuppy retina use an excitatory amino acid neurotransmitter. *Nature* 303, 537–538.

Tachibana, M. & Kaneko, A. (1984). γ-Aminobutyric acid acts at axon terminals of turtle photoreceptors: difference in sensitivity among cell types. *Proceedings of the National Academy of Science of the U.S.A.* 81, 7961–7964.

Watanabe, S.-I. & Murakami, M. (1985). Electrical properties of on–off transient amacrine cells in the carp retina. *Neuroscience Research* (Suppl.) 2, S201–S210.

Weiler, R. (1981). The distribution of center-depolarizing and center-hyperpolarizing bipolar cell ramifications within the inner plexiform layer of turtle retina. *Journal of Comparative Physiology A* 144, 459–464.

Yazulla, S. (1976). Cone input to bipolar cells in the turtle retina. *Vision Research* 16, 737–744.

Yazulla, S. (1986). GABAergic mechanisms in the retina. In *Progress in Retinal Research*, Vol. 5, ed. Osborne, N., pp. 1–52. Oxford: Pergamon.

Yazulla, S. & Studholme, K.M. (1990). Multiple subtypes of glycine-immunoreactive neurons in the goldfish retina: single and double-label studies. *Visual Neuroscience* 4, 299–309.